RV ARAON research activities within US EEZ waters in 2017

1. Research activities

Araon Arctic Cruise (ARA08AB) departed Incheon Korea, Alaska on July 21, 2017 and returned to Barrow on August 25, 2017 via Nome. With funding provided by the Ministry of Oceans and Fisheries (MOF) and by Korea Polar Research Institute (KOPRI), the aim of the cruise was to investigate the structure and processes in the water column and subsurface (sediment) around the Bering/Chukchi/Beaufort/East Siberian Seas in rapid transition. The research effort was the conducted research cruise of the Korea-Arctic Ocean Observing System (K-AOOS) Program with support from the MOF and the KOPRI. Total of 55 scientists and other staffs have participated from 11 countries (Korea, USA, China, Japan, France, Spain, Russia, Coatia, Italy, Germany, UK) representing 25 different universities and research organizations. Araon data were collected on the physical, biological, chemical, and biogeochemical properties the US EEZ waters (Fig. 1.1).

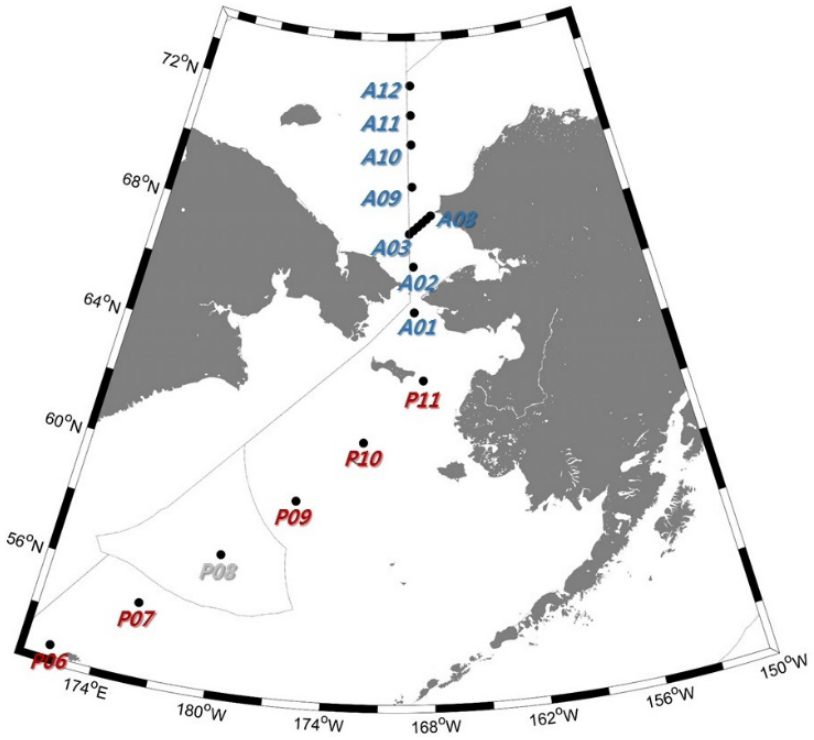

Figure 1.1. A station map of Arctic cruise (station P06, P07, P09 - P11 and A01 – A12). Black circles are study stations. Grey lines denote Russian EEZ and US EEZ lines. Work/transit in the US EEZ was performed during 30th July – 9th August 2017.

2. Materials and methods

1) Physical Oceanography

An intensive oceanographic survey with 12 hydrographic stations was conducted in the Chukchi Sea within US EEZ during the period of August 6 to August 9, 2017. Along the transect of hydrographic stations, vertical profiles of temperature, salinity, density, dissolved oxygen, fluorescence, transmissivity and PAR, and water samples were obtained from the hydro-casts of a SBE32 carousel water sampler equipped with a SBE9plus CTD profiler, a SBE43 dissolved oxygen sensor, a transmissometer, PAR and fluorometer, and 24 position rosette with 10-liter Nisken bottles. During the CTD upcasting, water samples were collected at several depths for biochemical analyses. For the precise reading, the salinities of collected water samples were further analyzed by an Autosal salinometer (Guildline, 8400B). The measurement was performed when the temperature of water samples was stabilized to a laboratory temperature, usually within 24-48 h after the collection.

2) Microbial Oceanography

During the Araon cruise in 2017, prokaryotic (i.e. Bacteria and Archaea) and viral abundances were measured at 7 stations (A01-A03, A06, A08, A10 and A12) within US EEZ waters. Samples were collected from 3-4 depths (surface to ca. 50 m) with 10 L Niskin bottles mounted on a CTD rosette. For measurements of viral and prokaryotic abundances, seawater samples (10 ml) were fixed with 0.02 μm filtered formalin (final conc. of 2%), and were stored at -80°C.

3) Phytoplankton ecology (Pigments and production)

The photosynthetic pigments and chlorophyll-a data were collected in the Chukchi Sea in 2017. A total of 12 stations were visited. Water samples were collected at 4-6 depths (Surface, 10m, 20m, 30m, 50m, and subsurface chlorophyll-a maximum depth) with a rosette sampler equipped with 10 L Niskin-type bottles, an in situ fluorometer, and a high-precision Sea-Bird plus CTD probe.

Subsamples from the Niskin bottles were filtered through a cascade connection of 20-μm

nylon mesh, Nuclepore filter (Whatman International) with pore size of 2 μm, and a Whatman GF/F filter to determine size-fractionated chlorophyll-a concentrations. Thus, micro (>20 μm), nano (2-20 μm), and pico-sized (<2 μm) chlorophyll-a concentrations could be measured directly. Subsamples for total chlorophyll-a were filtered onto 47 mm GF/F Whatman filters. Each filter was extracted in 90% acetone for 24 hours at 4 ºC in darkness, and chlorophyll-a concentrations were measured with a fluorometer (model Trilogy, Turner Designs, USA; method: Parson et al., 1984).

For photosynthetic pigments' analysis, 2 – 4 L seawater samples of surface and SCM layers were filtered onto 47 mm GF/F Whatman filters and stored at −80 °C. The filters were extracted with 3 mL 100 % acetone, ultrasonicated for 30 sec and maintained under 4 °C in dark for 15 hours. Debris was removed by filtering through 0.45 μm Teflon syringe filters. Just before injection, the extracts were diluted with distilled water to avoid the peak distortion of the first eluting pigments. Pigments were assessed by HPLC (Agilent series 1200 chromatographic system, Germany) with C8 column (Agilent XDB-C8, USA) following the method of Zapata et al. (2000).

To estimate carbon and nitrogen uptake of phytoplankton in the Chukchi and the East Siberian Seas, water samples were collected by CTD rosette at 6 different light depths (100, 50, 30, 15, 5, 1%) in 3 stations during this cruise (Station 2, 9, and 12). Productivity experiments were executed by incubating phytoplankton in the incubators on the deck for 4 hours with circulating surface seawater after stable isotopes (^{13}C, $^{15}NO_3$, and $^{15}NH_4$) as tracers were inoculated into each bottle. After the incubation, all productivity sample waters were filtered on 25mm GF/F filters for laboratory isotope analysis after this cruise. For the background data of the productivity stations, water samples were collected for alkalinity, macro nutrient concentrations (Nitrate, Nitrite, Silicate, Ammonium, and Phosphate), and total and size-fractionated (only for 100, 30, and 1% of light depth) chlorophyll-a concentrations.

4) Phytoplankton communities composition

The data were collected in the Bering Sea and Chukchi Sea from July 30 to August 9 in 2017. A total of 14 stations were visited. Water samples were collected at 4-6 depths (Surface, 10m, 20m, 30m, 50m, 100m, and subsurface chlorophyll a maximum depth) with a rosette sampler equipped with 20 L Niskin-type bottles, an in situ fluorometer, and a high-precision Sea-Bird plus CTD probe. The subsurface chlorophyll maximum layer

depths were estimated by CTD profiles. To analysis phytoplankton community composition, water samples were obtained with a CTD/rosette unit in 20 L PVC Niskin bottles during the 'up' casts. Aliquots of 125 mL were preserved with glutaraldehyde (final concentration 1%). Sample volumes of 50 to 100 mL were filtered through Gelman GN-6 Metricel filters (0.45 μm pore size, 25 mm diameter). The filters were mounted on microscopic slides in a water-soluble embedding medium (HPMA, 2-hydroxypropyl methacrylate) on board. The HPMA slides were used for identification and estimation of cell concentration and biovolume. The HPMA-mounting technique has some advantages over the classical Utermöhl sedimentation method. Samples were also collected via phytoplankton net tows (20 μm mesh) and preserved with glutaraldehyde (final concentration 2%); these samples were used only for identification of small species in the phytoplankton assemblage. Since the results from this can be biased towards larger specimens, these data were not used for statistical analysis, but only for morphological and systematic analysis

5) Macromolecular composition of phytoplankton

Particulate organic matter (POM) is composed of living and dead organisms, and refractory organic matter. Biochemical components of POM can be partitioned into fractions such as proteins (PRT), lipids (LIP), and carbohydrates (CHO). In case of POM as mainly phytoplankton-derived materials, biochemical composition of POM reflects the physiological state of phytoplankton in response to environmental conditions (Fabiano et al., 1993; Danovaro et al., 2000; Bhavya et al., 2018; Kim et al., 2018). Therefore, changes in biochemical composition of phytoplankton can be useful tool for physiological and nutritional condition as trophic resource.

Water samples for biochemical composition of POM obtained from 2~5 depths in euphotic layer. 0.5~1 L of each seawater sample went through a pre-combusted 25mm GF/F filter (pre-combusted at 450 °C, 4 hr) and then immediately stored at -80 °C until analysis. The fraction of PRT, CHO, and LIP were determined following the protocols (Lowry et al., 1951; Dubois et al., 1956; Bligh and Dyer, 1959; Marsh and Weinstein, 1966; Kim et al., 2015). Concentrations of macromolecules were measured using a spectrophotometer (Labomed, Germany), which is determined by comparison to the standard curve with blank filters (procedural control filters, Whatman GF/F filter).

6) Protozoa abundance, composition and grazing rates on phytoplankton

To determine the abundance and composition of protozoa, a CTD-Niskin rosette sampler was used to take water samples from the following 2-3 depths. For protozoa, 500 ml water from the vertical profiles was preserved with 1% acid Lugol's iodine solution these samples were then stored in darkness. For heterotrophic nanoflagellates and heterotrophic dinoflagellates smaller than 20 μm, 200 ml of water was preserved with glutaraldehyde (0.5% final concentration) and it was made with slide to analyze microscope. Grazing rates of heterotrophic protists on phytoplankton were determined by the dilution method (Landry and Hassett 1982). Water for grazing experiments was collected from 2 depths (surface, SCM) of each station, and gently filtered through a 200-μm mesh. At each station, 30L seawater were collected in a Niskin bottle and transferred to a polycarbonate carboy. Part of this water was filtered through the 0.22-μm filtration system. Dilution series were set up in ten 1.3-l PC bottles. Ten bottles were used to establish a nutrient-enriched dilution series consisting of replicate bottles with 20 and 100% natural seawater. The bottles were incubated on deck for 24-48h at ambient sea surface temperatures and screened to the ambient light level with neutral density screening. Subsamples were collected from replicate bottles at 0 and 24-48h to determine chlorophyll-a concentrations.

7) Mesozooplankton and Food web

Mesozooplankton samples were collected with bongo net (60 cm diameter, 330 and 500 μm mesh) at 14 selected stations. The bongo net was towed vertically within the upper 200 m of the water column for about 10 – 15 min. The depth sensor was attached to the net frame and the flow meter was located in the center of net to estimate the volume of seawater. Samples from 330 μm were immediately fixed and preserved with 10% neutralized formaldehyde for the quantitative analysis and samples from 500 μm were used to find the dominant zooplankton species with microscope and frozen at -80 oC for the post analysis. The samples preserved with formaldehyde were split with a Folsom splitter into the sub-samples of about 1,000 individuals for taxonomic identification and counting in the laboratory. Each species abundance was quantified by the revolution

counts of a flow meter attached to the center of the net mouth.

Also, we used stable carbon and nitrogen isotopes to investigate whether drastic changes in species composition also cause changes in food web structure and to identify the main trophic pathways and main food sources that support the meso-fauna assemblages in these systems. Especially, we focused the zooplankton organisms, especially copepods, associated with the pelagic food webs. To estimate food wed interactions, the surface waters of survey stations were filtered on GF/F filters (Whatman, 0.7 μm pore, ø = 25 mm) and frozen at –20 °C for the post analysis. And, the zooplankton samples from bongo net were immediately sorted on board and kept frozen (–20 °C). The organisms, which sorted on the microscope (Nikon SMZ 1500), were identified to the lowest taxonomic level (i.e. generally at the species level).

Figure 1.7.1. Zooplankton collector Bongo-net

8) Ocean Optical Observation

In this cruise, we tried to obtain bio-optical relationships to improve ocean color data quality by observing absorptions from phytoplankton, suspended sediment (SS), inherent optical properties (IOPs) of water (e.g. absorptions by colored dissolved organic matters (CDOM)) and apparent optical properties (AOPs) of water (e.g. downwelling irradiances (Ed) and upwelling radiance (Lu)). Our major goal in this study was to collect bio-optical data in conjunction with measurements of CDOM, phytoplankton and SS absorption in support of NASA's efforts to develop robust empirical and semi-analytic algorithms for ocean color products in high latitude regions. This effort is a part of longer strategic objective of understanding the impacts of changing climate on biological oceanographic processes in the Arctic Ocean using ocean color satellite data.

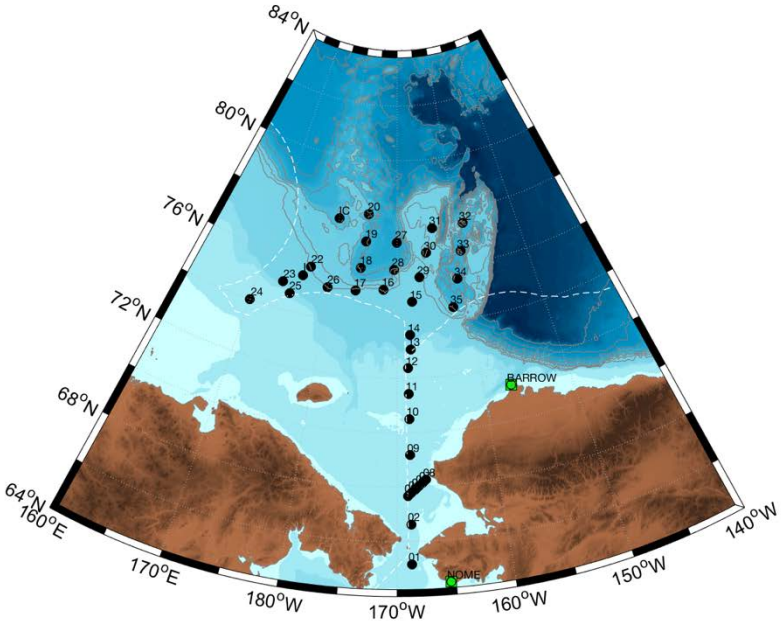

Figure. 1.8.1. A station map for ocean optical observation

We sampled 36 waters at 12 stations (with 3 depths of surface, subsurface chlorophyll maximum, and bottom within euphotic depth) and 9 intermediate sites between stations in underway route (Fig. 1.8.1). To measure inherent optical properties (IOPs) of water, seawater volumes of 500 - 2,000 ml were filtered on 25 mm glass-fiber filters. Optical densities of total particulate matters were measured directly on the wet filters by methods of Truper and Yentch (1967) with a double-beam recording spectrophotometer (Cary100, Agilent Technologies) in a spectral range 250 - 800 nm (spectrum resolution of 1 nm). The filter was placed in front of diffusing windows adjacent to an end-on photomultiplier

of large surface area. For a reference blank and baseline variations, an unused wetted filter was used, and the instrument was taken as were automatically corrected. After the measurement of optical density of total pigments, the spectral absorption by non-algal material was measured separately with the method of Kishino et al. (1985).

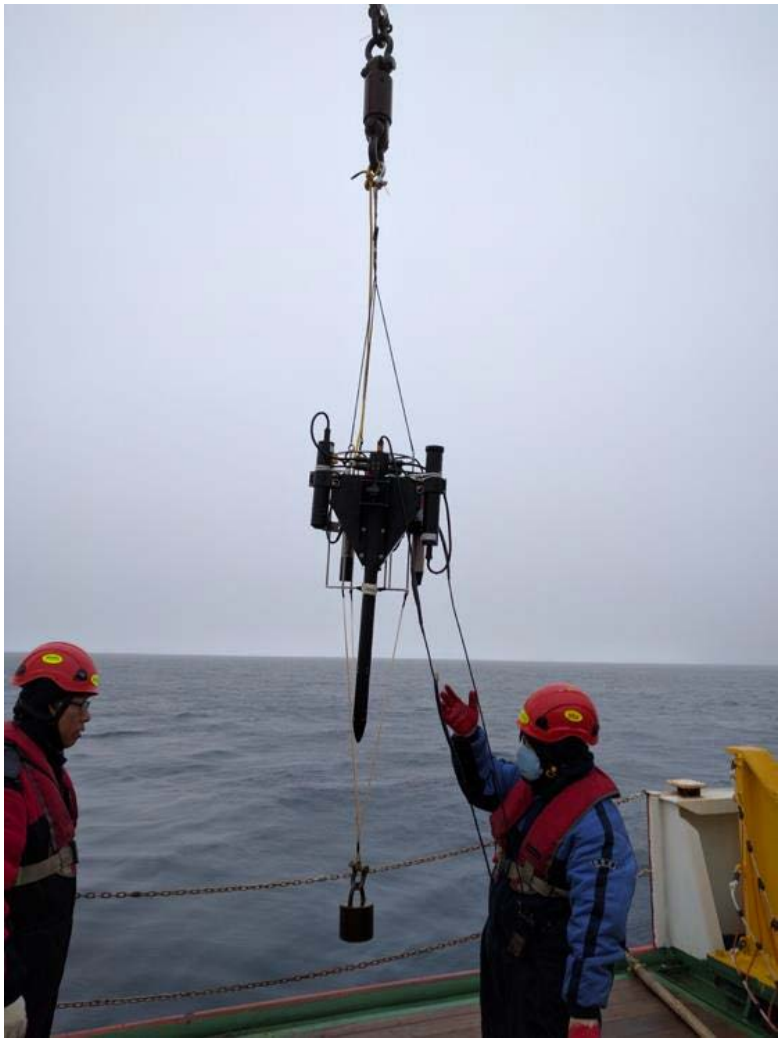

Figure. 1.8.2. Deploy of hyper-spectrometer (HPRO II).

For the measuring apparent optical properties (AOPs) of water, we deployed hyper-spectrometer (HPRO II, Fig. 1.8.2) with a spectral range of 350 - 800 nm (HPRO II) of downwelling irradiance (Ed) and upwelling radiance (Lu). For the reference as ambient irradiance variation, downwelling irradiance (Es) was measured on deck in a place without shade. The integrated instruments deployed through the A-frame at the stern of the vessel. The deploying speed was 10 m/min. This data will be able to be used for calibrations and validations of currently operating ocean color remote sensing data.

9) Phytoplankton physiology (photochemistry)

To investigate the impact of physico-chemical conditions on photosynthesis in the study area, we measured photosynthetic characteristics of phytoplankton at total 12 stations using a Fluorescence Induction and Relaxation (FIRe) system (Fig. 1.9.1). Continuous measurements also conducted on underway (using pumped on seawater around 7 m depth beneath the ship) during the Araon transit. Active fluorometry is a non-destructive and rapid method, and it has been used to monitor variations in the photochemistry (Kolber and Falkowski, 1993; Falkowski and Kolber, 1995). These measurements provide an express diagnostics of the effects of environmental factors on photosynthetic processes such as nutrient limitation. After collection from Niskin bottles at 5 - 6 depths within 100 m, samples were kept under in situ temperature in light bottles. These samples were measured after 30 - 60 minutes low light adaptation. Photosystem II (PSII) parameters such as the minimal fluorescence yield (F_0; when all reaction centers are open), the maximal fluorescence yield (F_m; all reaction centers are closed), the quantum efficiency of PSII (F_v/F_m), the functional (or effective) absorption cross-section of PSII (σ_{PSII}) were measured as describe in Kolber et al. (1998). Quantum efficiency of photochemistry in PSII (F_v/F_m) was calculated as a ratio of variable fluorescence ($F_v = F_m - F_0$) to the maximum one (F_m). The fluorescence measurements were corrected for the blank signal recorded from filtered seawater by 0.2 um syringe filter set.

Figure 1.9.1. A custom-built Fluorescence Induction and Relaxation (FIRe) system onboard Araon.

10) UV absorbing compound (Mycosporine-like amino acids; MAAs) and light intensity

Through direct exposure to incoming solar radiation and enhanced back scatter associated with the high albedo of surrounding sea ice, surface melt ponds are exposed to the highest light intensity (Perovich, 2006; Ehn et al., 2011; Nicolaus et al., 2012). Among species photoinhibition is variable protective strategies. To protect against the detrimental effects of UV radiation many microalgae produce mycosporine-like amino acids (MAAs), which are a group of small water-soluble compounds, have absorbed the UV wavelength (Shick and Dunlap, 2002). The aim of this research is to provide the distribution of MAAs as fundamental information of EEZ marine ecosystem and understand the photoprotection of phytoplankton.

a) UV absorbing compound (Mycosporine-like amino acids)

MAAs were extracted and calculated according to Ha et al. (2014). To analyze the MAA contents in water samples, 3-4 L of each sample was filtered through pre-combusted (450°C, 4 h) glass fiber filters (47 mm) and stored at -80°C until analysis. A 3 mL volume of 100 % methanol was then added to the samples, and an ultrasonicator (30 s, 50 W; Ulsso Hi-Tech: Seoul, Korea) was used to disrupt them. The samples were next placed in a freezer at 4 °C over-night, after which the solvent phase was transferred to a 2 mL microtube through a 0.2 μm syringe filter (PTFE 0.2 μm Hydrophobic). A centrifugal evaporator (CVE-200D; EYELA) was employed to completely dry the solvent. The dried sample was then dissolved in 500 μL of distilled water, and 100 μL of chloroform was added to remove lipids and pigment. The sample was subsequently centrifuged for 10 min at 10,000 rpm. A 400 μL aliquot of the supernatant was finally separated and injected into a HPLC (Agilent Technologies, 1200 series, Wilmington, DE, USA) to quantitatively analyze the MAA contents.

b) Light intensity

To estimate the penetration of UV-B, UV-A, and PAR in the water column, radiation was measured by RMSES radiometer (TriOS GmbH, Germany) at each sampling stations. We measured the radiation from surface to 40 m the UV-B (280 nm - 320 nm), UV-A (320 nm360 nm), and PAR (400 nm - 700 nm) as the intensity (W m^{-2}).

11) Nutrients and dissolved and particulate organic carbon and nitrogen in the Arctic Ocean

Seawater sampling for nutrients (PO_4, NO_2+NO_3, NH_4, and Si(OH)4), dissolved organic carbon and nitrogen (DOC and DON) and particulate organic carbon and nitrogen (POC and PON) was carried out at 18 stations in the subarctic western North Pacific and Chukchi Sea using a CTD/rosette sampler holding 24-10 L Niskin bottles (SeaBird Electronics, SBE 911 plus) during Korea research ice breaker R/V Araon cruise (ARA08B, July 30–August 9, 2017) (Fig. 1.1).

a) Nutrients

Samples for nutrients were collected from the Niskin bottles into 50 ml conical tubes and immediately stored in a refrigerator at 4°C prior to chemical analyses. All nutrients samples were analyzed onboard within 3 days. Concentrations of nutrients were measured using standard colorimetric methods adapted for use on a 4-channel continuous Auto-Analyzer (QuAAtro, Seal Analytical). The channel configurations and reagents were prepared according to the 'QuAAtro Applications'. Standard curves were run with each batch of samples using freshly prepared standards that spanned the range of concentrations in the samples. The r2 values of all the standard curves were greater than or equal to 0.99. In addition, reference materials for nutrients in seawater (RMNS) provided by 'KANSO Technos' (Lot. No. 'BV') were used along with standards at every batch of run in order to ensure accurate and inter-comparable measurements.

b) Dissolved organic carbon and nitrogen

For DOC and DON measurements, seawater sample was drawn from the Niskin bottle by gravity filtration through an inline pre-combusted (at 550°C for 6 hours) Whatman GF/F filter held in an acid-cleaned (0.1 M HCl) polycarbonate 47 mm filter holder (PP-47, ADVANTEC). The filter holder was attached directly to the Niskin bottle spigot. The filtrate was collected in an acid-cleaned glass bottle and then distributed into two pre-combusted 20 ml glass ampoules with a sterilized serological pipette. Each ampoule was sealed with a torch, quick-frozen, and preserved at –24°C until the analysis in our land laboratory. Analyses of DOC and DON were performed by high temperature combustion using a Shimadzu TOC-L analyzer equipped with an inline

chemiluminescence nitrogen detector (Shimadzu TNM-L). Milli-Q water (blank) and consensus reference material (CRM, 42–45 μM C, deep Florida Strait water obtained from University of Miami) were measured every sixth analysis to check the accuracy of the measurements. The precision of the DOC measurements was 2–3 μM or a CV of 3–5%.

c) Particulate organic carbon and nitrogen

For determination of POC and PON, seawater sample was drawn from the Niskin bottle into an amber polyethylene bottle. Known volumes (2 L) of seawater were filtered onto pre-combusted Whatman GF/F filters (25 mm) using a filtering system under gentle vacuum at < 0.1 MPa. To prevent data scattering, large zooplankton (e.g., copepods) were removed from the filter samples using tweezers after washing with filtered seawater if they were captured on the filters. These filter samples were stored at –80°C until the analysis in our land laboratory. Before POC analyses, the filter samples were freeze-dried, and then exposed to HCl fumes for 24 h in a desiccator to remove inorganic carbon from the samples. Measurements were carried out with a CHN elemental analyzer (vario MACRO cube, Elementar, Germany). Acetanilide was used as a standard. The precision of these measurements was ± 1.0 μmol L^{-1}.

12) Atmospheric black carbon and chemical properties of aerosols

Atmospheric black carbon (BC) monitoring and aerosol sampling were conducted on board the Korean icebreaker IBR/V Araon over the subarctic western North Pacific and Chukchi Sea during the cruise (ARA08B, July 30–August 9, 2017) using a continuous soot monitoring system (COSMOS, Model 3130, KANOMAX) and two high-volume aerosol samplers (HV-100R, Sibata Scientific Technology Ltd.), respectively. A total of 5 aerosol samples were collected during the cruise.

a) Black carbon

Air intake was set at the handrail of the front deck to avoid contamination from the ship’s exhaust (Fig. 1.12.1). Air sample was continuously pumped into the laboratory through a sampling tubing. We attached a cyclone at the intake to selectively sample PM2.5 aerosols. The flow rate of air samples was kept at 10 L/min in total to maintain the cyclone’s performance. A part of air flow (0.9 L/min) was introduced into the BC monitor.

A continuous soot monitoring system (COSMOS, MODEL 3130, KANOMAX) was used for fully automated, high-sensitivity, continuous measurement of light absorption by black carbon (BC) aerosols (Fig. 1.12.1). The instrument monitors changes in transmittance across an automatically advancing quartz fiber filter tape using an LED at a 565 nm wavelength. To achieve measurements with high sensitivity and a lower detectable light absorption coefficient, COSMOS uses a double-convex lens and optical bundle pipes to maintain high light intensity and signal data are obtained at 1 min. In addition, sampling flow rate and optical unit temperature are actively controlled. The inlet line for COSMOS is heated to 400 degrees C to effectively volatilize non-refractory aerosol components that are internally mixed with BC.

In addition to BC, ozone (O_3) was measured by ultraviolet (UV) absorption spectroscopy (Fig. 1.12.2). Briefly, ambient air was continuously drawn from an air sampling inlet, and then directed to the O_3 instrument by means of a passivated Teflon tubing. The mixing ratios of O_3 were determined using photometric instruments based on absorption in the ultraviolet region. The O_3 instrument utilized absorption at 253.7 nm emitted by a low-pressure mercury lump (Dylec Inc., Model 1100). The ambient O_3 data was used to scrutinize the data contaminated by the ship's exhaust, and to characterize the air masses observed during the cruise. When the O_3 mixing ratios were very low (i.e., 0 ppbv), it is very likely that the air sampled was contaminated by the ship's exhaust. Even if the O_3 mixing ratios were not very low but moderately low (i.e., 10-20 ppbv), it is likely that the air sampled was affected by the ship's exhaust to some extent. In this work we used the threshold of 20 ppbv O_3 to filter the BC data for clean air that were not affected by any contamination by the ship.

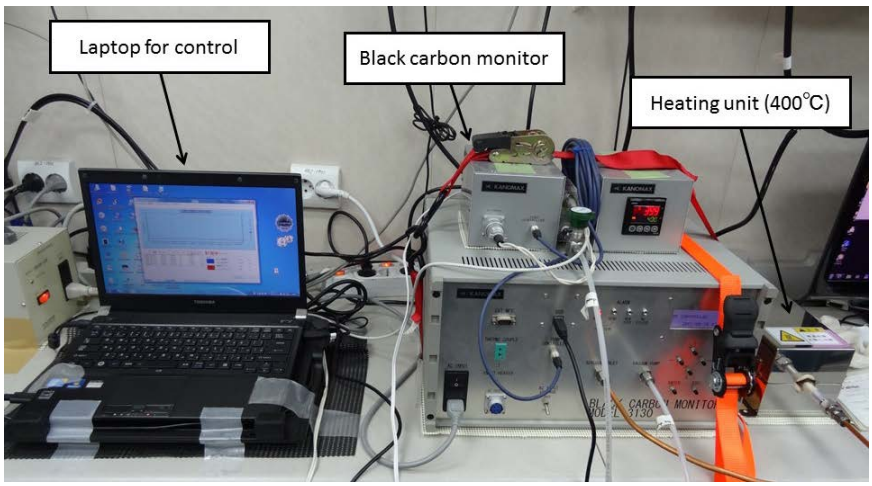

Figure 1.12.1. Inlet and instruments for measuring black carbon in air.

Figure 1.12.2. Instruments for measuring ozone in air.

b) Aerosol sampling

During the cruise, two high-volume aerosol samplers (HV-100R, Sibata Scientific Technology Ltd., Tokyo, Japan) were located at the upper deck of the ship and used to collect marine aerosols on pre-combusted (at 550°C for 6 h) quartz filters (25 X 20 cm, QR-100, Sibata Scientific Technology Ltd.) at a sampling flow rate of 1000 L/min (Fig. 1.12.3). To collect fine (D < 2.5 μm) and coarse modes (2.5 μm < D < 10 μm) aerosols on the filters, particle size selector for PM2.5 and PM10 were installed to each aerosol sampler. Possible contamination from ship exhaust was prevented by using a wind-sector controller during the cruise. The wind-sector controller was set to collect marine aerosol samples only when the relative wind directions were within plus or minus 100° relative to the ship's bow and the relative wind speeds were over 1 m/s. The sampling time for each sample was approximately 48 hours. During the cruise, a total of 5 samples were collected. After sampling, the filters were stored frozen at –24°C before chemical analysis. Until now, chemical analyses for ions, water-soluble organic carbon and nitrogen (WSOC and WSON), total carbon and nitrogen (TC and TN) were not conducted.

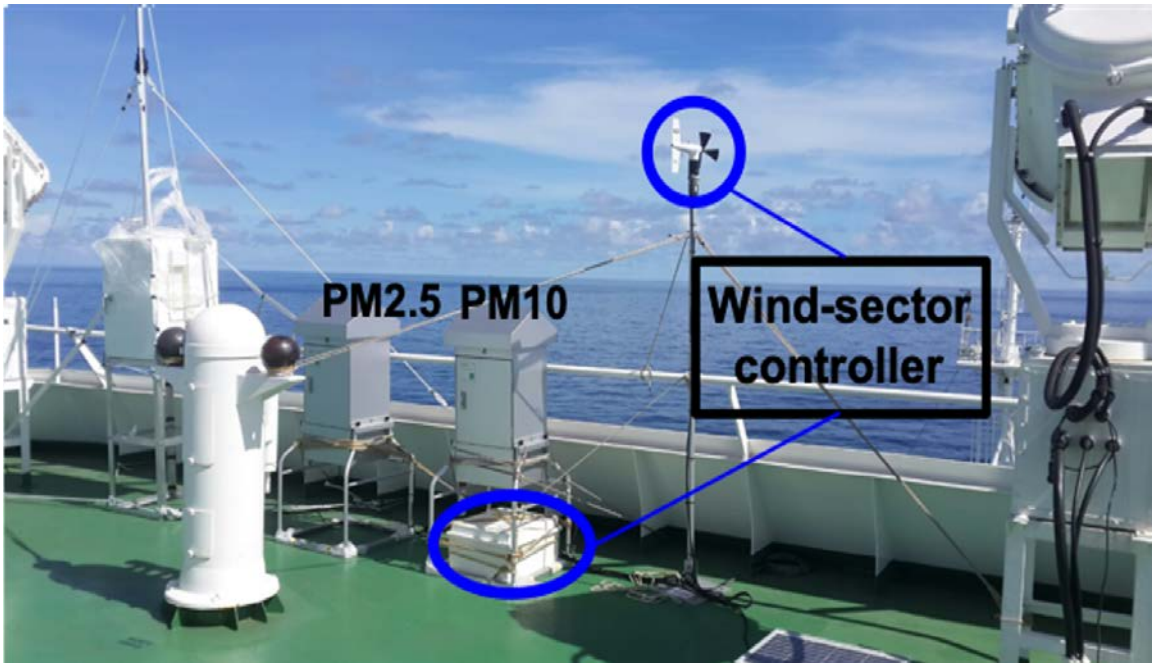

Figure 3. High-volume aerosol samplers and a wind-sector controller system.

13) Air-sea CO_2 exchange and water column carbonate system

CO_2 flux across the sea surface is usually determined by the concentration difference between the dissolved CO_2 in the surface mixed layer and the atmospheric CO_2 overlying the surface with a parameterized gas transfer velocity k. Dissolved CO_2, so called pCO_2, was determined using an aqueous and gaseous phase equilibration technique with a small Weiss-type equilibrator. The air above the surface was withdrawn from the intake cup mounted at the foremast at 29 m above sea-level. The CO_2 in the air and the equilibrator headspace was analyzed with Li-cor 7000 in which 4.5 um wavelength of photon is selectively absorbed by CO_2. The analyzing system was calibrated every 6 hours using a series of calibration gases and one zero air. pCO_2 in the seawater was acquired every minute in a computer and atmospheric CO_2 every 6 hours. The raw data was corrected for the effect of temperature difference between the in-situ and the equilibrator after coming back to the institute, and gas transfer velocity was determined using parameterization with wind speed which has been logged in DADIS onboard Araon.

Carbonate system in the water column compose of ionic form of carbonate (CO_3^{2-}), bicarbonate (HCO_3^-), hydrogen ion (hydronium) and neutral form of carbonic acid and dissolved CO_2. These carbonate species exist in equilibrium in seawater depending on

alkalinity of the seawater. These species, however, cannot be analyzed directly using analytical instruments except CO_2 and hydronium. Thus, to determine the carbonate system in the water column, we measure total dissolved inorganic carbon (DIC) and total alkalinity (TA) by which one can derive ionic and neutral form of carbonate system. DIC and TA are defined as follows:

$$DIC = [HCO_3^-] + [CO_3^{2-}] + [CO_2] + [H2CO_3]$$

$$TA = [HCO_3^-] + 2[CO_3^{2-}] + \Sigma\,[anions] - \Sigma\,[cations]$$

DIC and TA were analyzed in the laboratory after collecting seawater samples aboard at the hydrographic stations. To prevent the seawater samples from being altered due to biological activities in the seawater, 100 uL of $HgCl_2$ solution (50%) were injected upon collecting the samples from the Niskin seawater collected attached in CTD/Rosette. The sample bottles were flushed 3 times before starting collection in 250 mL bottle. Making small headspace, injecting $HgCl_2$ solution, and tightening the lid with black electric tape, the samples were stored in a dark place before analysis.

We also collect seawater samples for analysis of pH onboard. The procedure of collection is the same as that for DIC and TA.

To analyze dissolved CO_2 in the water column, a specially designed bottle was employed to avoid contact with ambient air onboard. The bottle composes of one stopcock and septum lid on both sides. Seawater flows through these two ends and the body of the bottle which was upright overflowing a certain time period to flush the bottle and to get rid of any bubbles inside. Upon collecting the seawater, 50 mL of CO_2 free N_2 gas was injected into the jar to equilibrate it with the water in. The equilibrated headspace air was then analyzed onboard or in the laboratory. 40 uL of $HgCl_2$ was injected to avoid contamination from biological activities.

14) Investigation of the microplastic contamination in surface water

a. Microplastic

During the cruise of R/V ARAON in 2017, sampling was carried out to investigate microplastic contamination in surface water at eight stations in the US EEZ. Surface samples were collected using a manta trawl (1 m wide; 0.34 m height, 0.200 mm mesh,

3.5-m length). The net was towed in a straight line to the next station from a previous station for 20minutes at an average speed of 2 knots. A calibrated flow meter was attached to the mouth of the net for calculation of the amount of water filtered. Water volume collected ranged from 225.5 to 502.7 m^3 with depending on the condition of tide and wave. To avoid potential contamination, all connecting lines including manta net frame-to-winch and flow meter-to-net frame were replaced by a stainless-steel wire. Dishes and washing were prohibited to prevent the outflow of wastewater from two hours before manta trawling. After towing, the net was returned to the stern of the vessel where is was rinsed from the outside with a deck hose. The cod-end was removed and taken to the laboratory where it was rinsed and filtered into stainless steel sieve (200 μm) to reduce the volume (about 200 ml). The filtered samples were transferred to a 1-L glass wide-mouth jar and stored in formalin (4% final concentration) for analysis.

b. Chemical pollutant

We had included the collection of samples for styrene oligomers (SOs) analysis in our original plan. However, we did not collect sample for that, depending on in situ condition.

15) Nitrogen source determination using nitrogen isotope of amino acids

Samples were collected in 18 stations which include the Bering Strait and the Western North Arctic. We collected those samples below.

Type	Analysis
Seawater	Oxygen isotope ratio ($\delta^{18}O$)
Particulate organic matter	Carbon ($\delta^{13}C$) and nitrogen isotope ratio ($\delta^{15}N$)
Zooplankton	Bulk tissue of nitrogen isotope ratio ($\delta^{15}N$) Nitrogen isotope ratio of amino acids ($\delta^{15}N_{AAs}$)

16) Atmospheric Observations

Atmospheric observations on IBRV Araon include the basic surface meteorological

parameters (e.g., air temperature, humidity, pressure and wind) and aerosols. All the observations were almost continuous during the cruise, so we obtained various time series along the cruise track. However, CO_2 concentrations were not observed because the eddy-covariance system was not loaded on the ship.

Meteorological observations on the radarmast include air temperature and relative humidity (HMP45D, Vaisala, Finland), air pressure (PTB100, Vaisala), and horizontal winds (2D sonic anemometer). The data logger (CR3000, Campbell Scientific, Inc., USA) scans each sensor every 10 seconds and saves the average of scans every 10 minute.

3. Scientific achievements

1) Physical Oceanography

a. Vertical Structures

Vertical structures of potential temperature and salinity at the transection from St. 1 to St. 12 are shown in Figs.3.1.1 and 3.1.2 (other parameters are plotted in Figs. 3.1.3, 3.1.4, and 3.1.5). The Pacific Water around the Bering Strait (St. 1) is specified with 3-10 °C and 32.0-32.5 psu. Temperature difference between bottom and surface is nearly 7~8 °C at St. 1. From St. 3 to St. 6, the cold water seems to inflow from the west and prevent the warm water to be extended from the Alaskan coast. From St. 7 to St. 8, relatively warm and fresh water inflows from the west. It appears that the Alaskan Coastal Water (warm and fresh) inflowing along the coast via Bering Strait makes clockwise eddy and then re-flows toward the east (coast). From St. 9 to St. 11, relatively warm water exists on the upper layer (8~9 ^{o}C). As sea ice meltwater exists on the high latitude from St. 12 (Fig. 3.1.4), surface water represents relatively low temperature (~ 4 ^{o}C) and relatively low salinity (~30.4 psu).

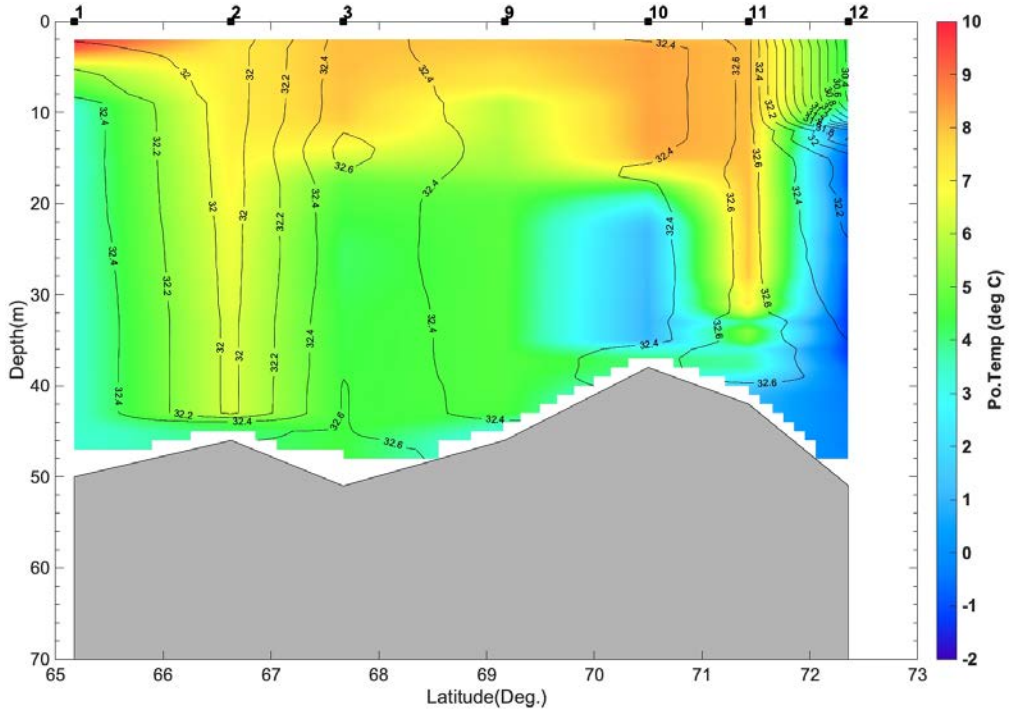

Fig. 3.1.1. Vertical structures of potential temperature and salinity at the transection from St.1 to St.12.

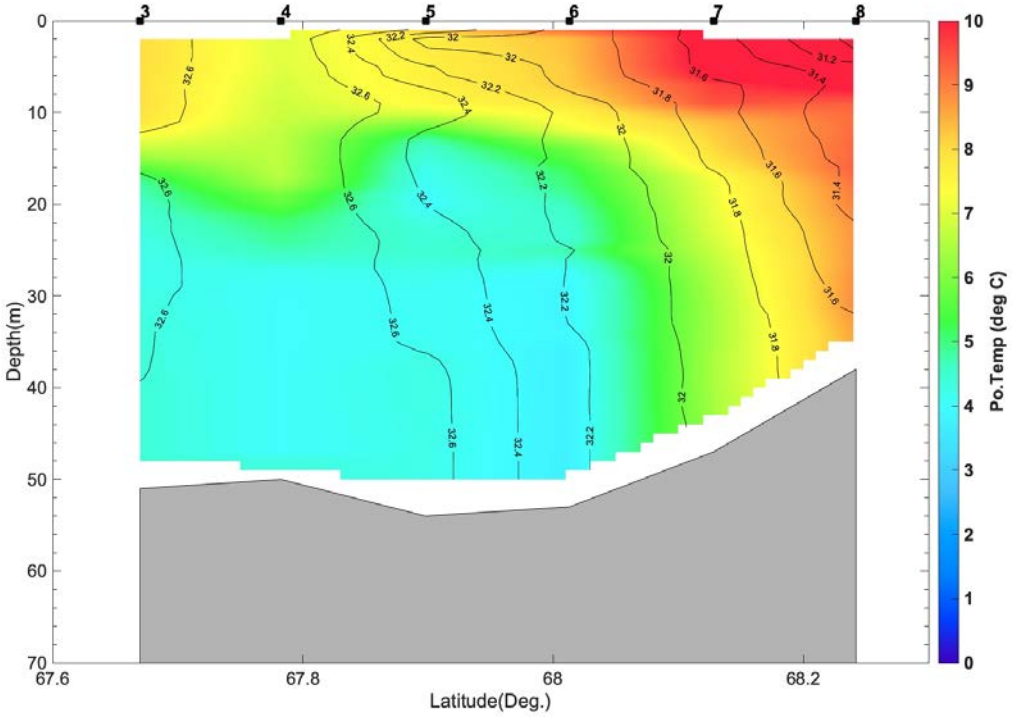

Fig. 3.1.2. Vertical structures of potential temperature and salinity at the transection from St.3 to St.8.

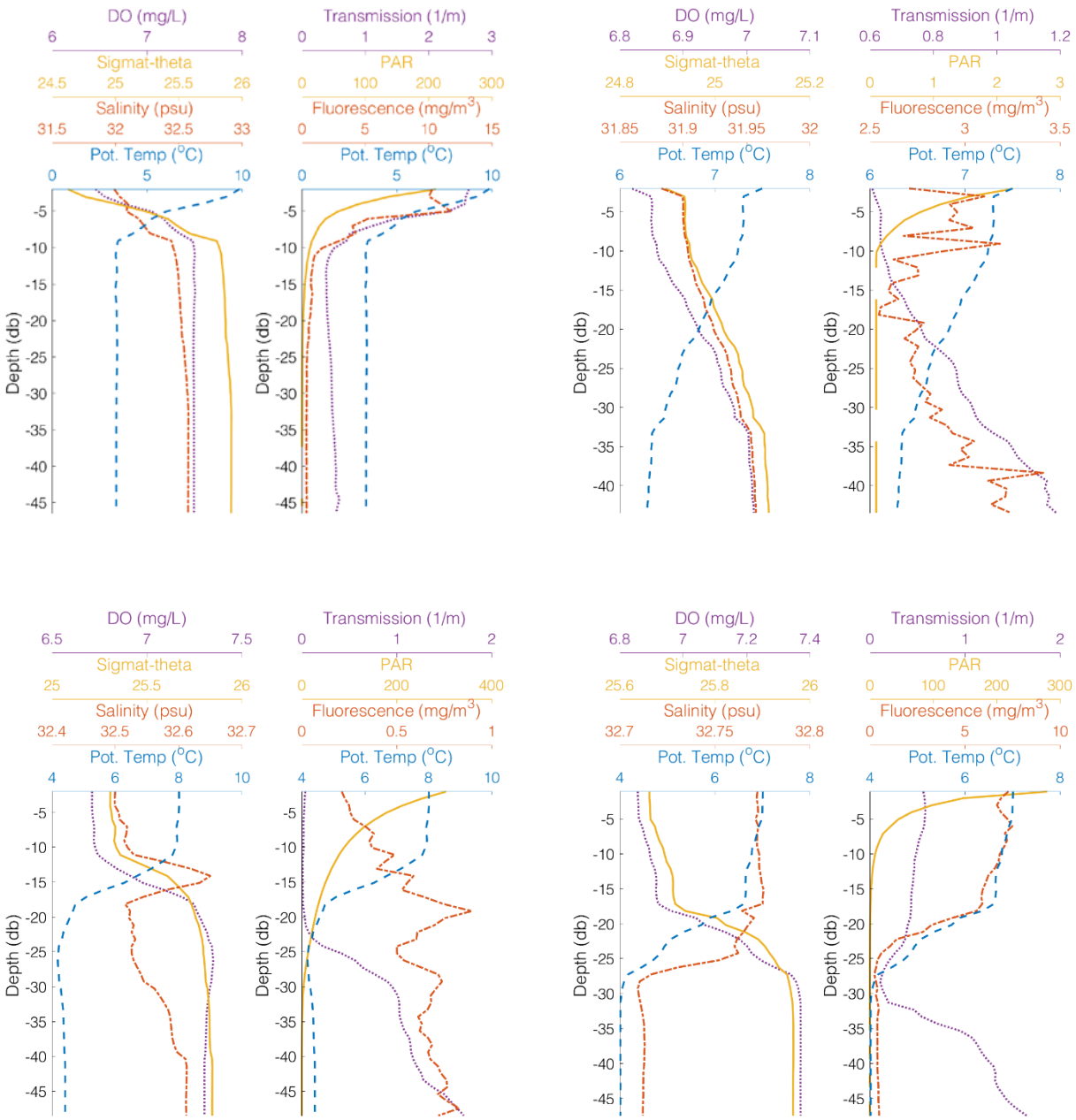

Fig. 3.1.3. Vertical structures of oceanographic parameters (potential temperature, salinity, density, dissolved oxygen, fluorescence, PAR, and transmission) from St.1 to St.4.

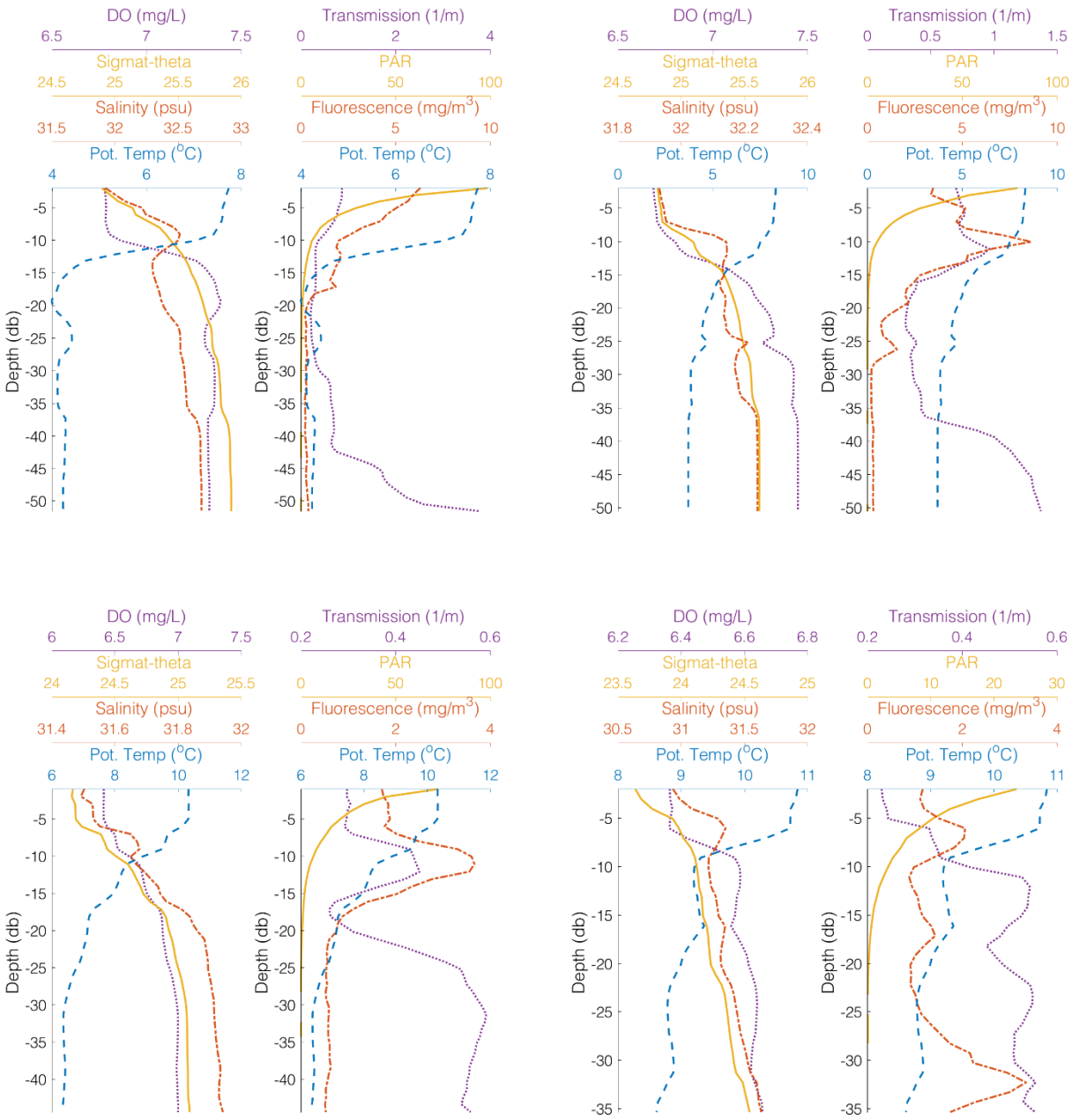

Fig. 3.1.4. Vertical structures of oceanographic parameters (potential temperature, salinity, density, dissolved oxygen, fluorescence, PAR, and transmission) from St.5 to St.8.

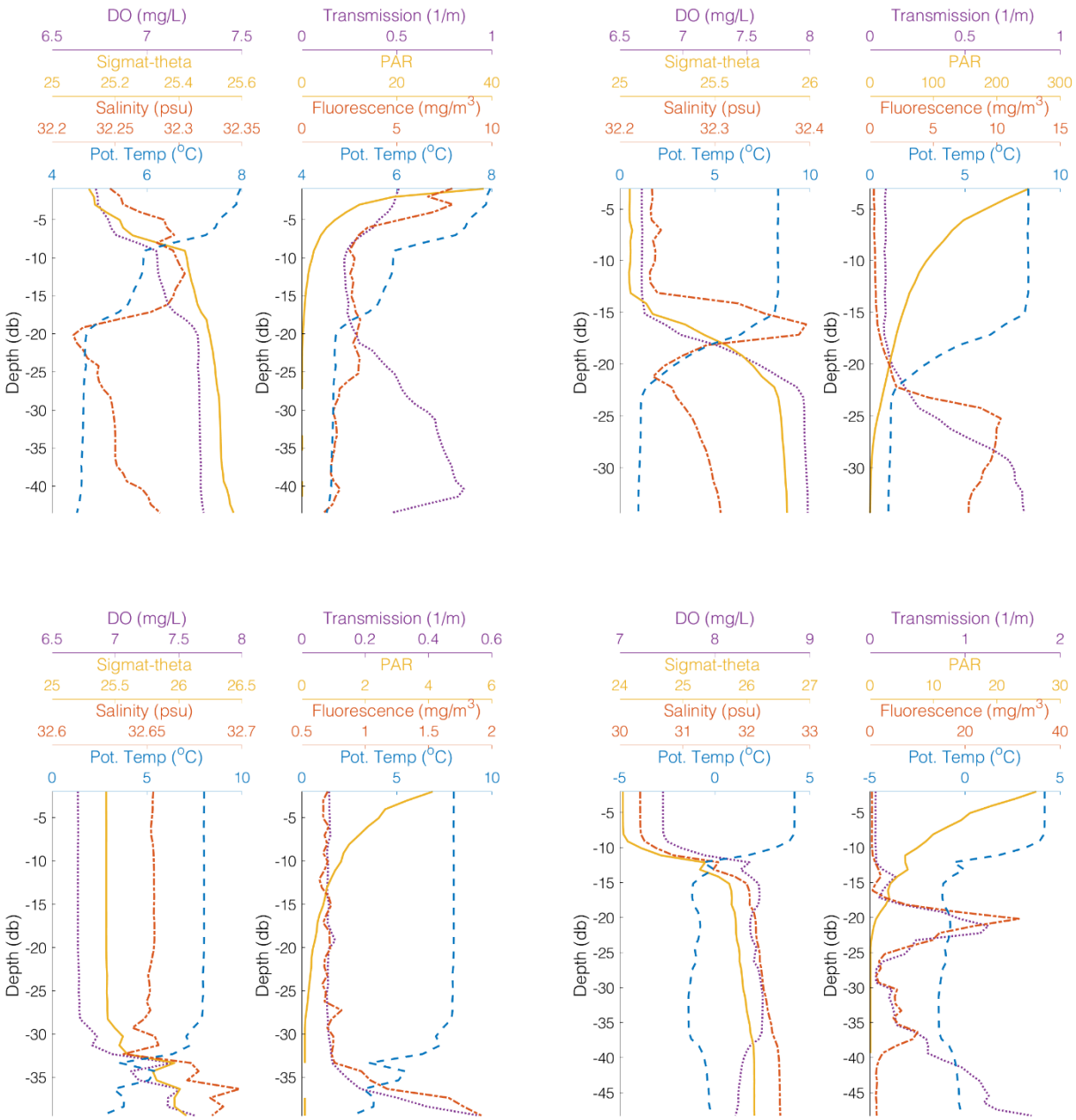

Fig. 3.1.5. Vertical structures of oceanographic parameters (potential temperature, salinity, density, dissolved oxygen, fluorescence, PAR, and transmission) from St.9 to St.12.

2) Microbial Oceanography

Prokaryotic populations ranged from 0.4-5.9 × 10^6 cells ml^{-1} and virus populations ranged from 0.2–1.6 × 10^7 viruses ml^{-1}. Further analysis is in progress.

3) Phytoplankton ecology (Pigments and production)

The photosynthetic pigments and chlorophyll-a concentrations were determined in the US EEZ waters during August 2017. A total of 12 stations were visited and water samples were collected at 4-6 depths at each station including subsurface chlorophyll-a maximum layer.

The chlorophyll-a concentration varied from 0.25 to 10.83 μg/L with an average of 2.03 μg /L in this region (Fig. 3.3.1). The depth-averaged chlorophyll-a concentration was the highest at station 4 and the lowest at station 3. The micro- (>20μm) and pico- (<2μm) size chlorophyll-a concentrations made the highest and lowest contribution to total chlorophyll-a content, respectively 72.1% and 20.1% on average, indicating the large contribution of micro- and nano-size phytoplankton to primary production in this region. The subsurface chlorophyll-a maximum layer became developed between surface to 40m depth.

The detected photosynthetic pigments of phytoplankton were chlorophyll-a, -b, -c2, -c3, fucoxanthin, alloxanthin, 19'-butanoyloxyfucoxanthin, prasinoxanthin, violaxanthin, 19'-hexanoyloxyfucoxanthin, diadinoxanthin, diatoxanthin, zeaxanthin, ββ-carotene, and the degradation products of chlorophyll.

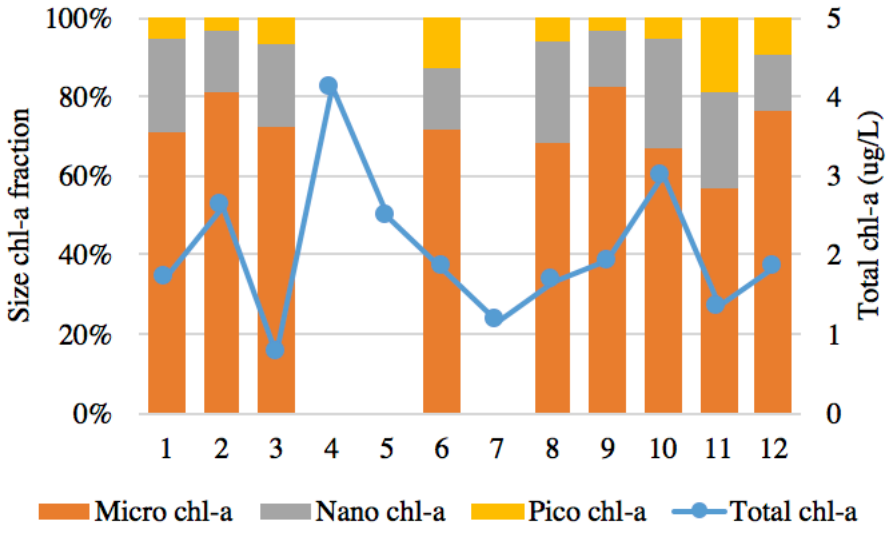

Figure 3.3.1. The surface chlorophyll-a concentrations (μgL^{-1}) and size-fractionated chlorophyll-a fractions (%) in August 2017.

To investigate the spatial distribution of the primary production and new production of phytoplankton, seawater samples were collected in the 6 light depths (100, 50, 30, 15, 5, 1%) at station 2, 9, 12. Then, the carbon uptake rates and the nitrate uptake rates were measured by using dual stable isotope tracers (^{13}C, $^{15}NO_3$).

The integrated carbon uptake rates of phytoplankton in euphotic layer ranged from 42.12 mg C m^{-2} h^{-1} to 85.53 mg C m^{-2} h^{-1} with and average of 60.97 mg C m^{-2} h^{-1}. The integrated nitrate uptake rates ranged from 2.00 mg N m^{-2} h^{-1} to 13.96 mg N m^{-2} h^{-1} with an average of 6.71 mg N m^{-2} h^{-1}. The highest carbon uptake rate was observed in the station 9 and the lowest carbon uptake rate was observed in the station 12 (Fig. 3.3.2). The highest and the lowest nitrate uptake rates also were observed in the station 9 and 12, respectively (Fig. 3.3.2).

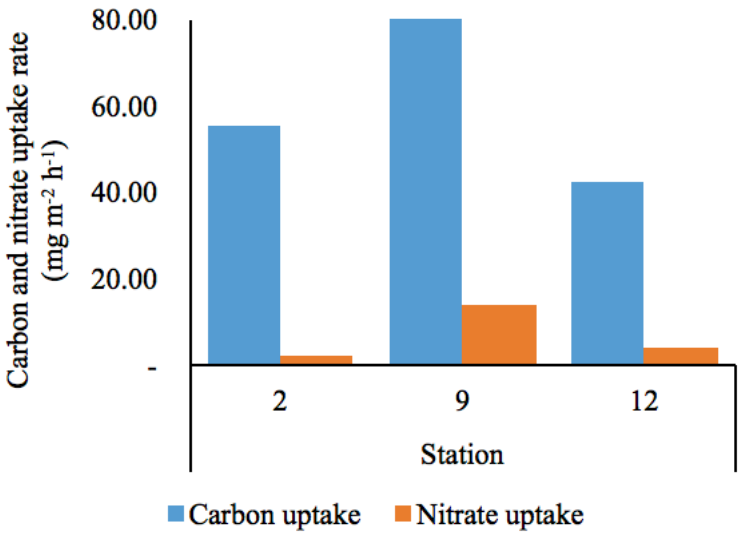

Figure 3.3.2. Spatial distribution of the carbon and nitrate uptake rates of phytoplankton integrated in the euphotic layer.

4) Phytoplankton communities composition

Based on the HPMA slide method and SEM analysis, the samples were made for identifying species compositions of phytoplankton later at the laboratory in KOPRI (Fig. 3.4.1)

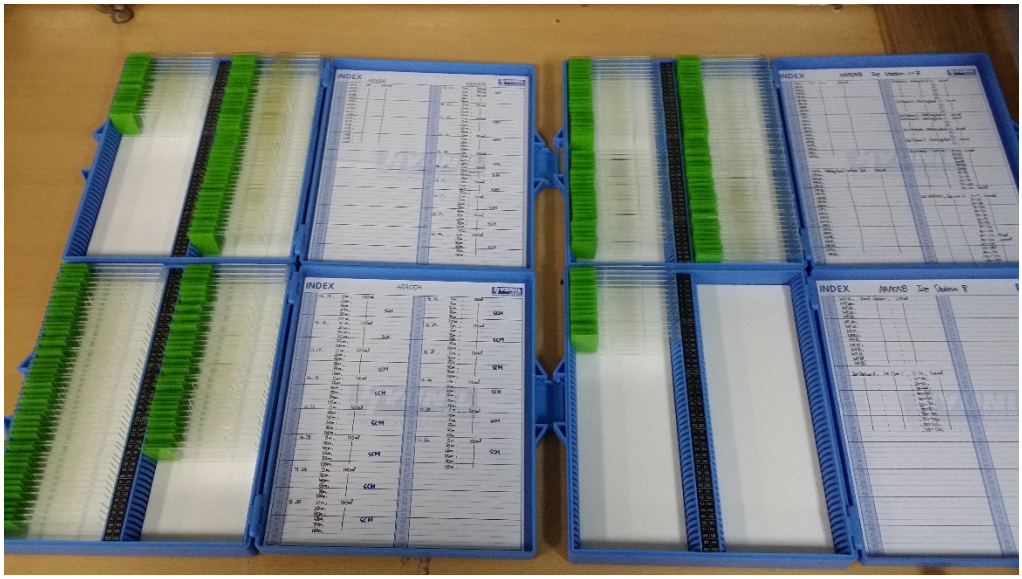

Figure. 3.4.1 HPMA Slides for Quantity analysis of phytoplankton communities.

5) Macromolecular composition of phytoplankton

The LIP and PRT concentrations in phytoplankton ranged from 13.6 to 183.1 µg L-1 (mean ± SD = 64.3 ± 50.5 µg L^{-1}) and 32.5 to 573.8 µg L^{-1} (mean ± SD = 133.6 ± 135.7 µg L^{-1}) within euphotic layer, respectively (Fig. 3.5.1). The CHO concentration, ranging from 48.4 to 761.6 µg L^{-1} with a mean of 207.2 µg L^{-1} (SD = ± 174.6 µg L^{-1}) (Fig. 3.5.1). Overall, CHO accounted for 59.9% of phytoplankton for all survey stations in EEZ, followed by PRT (33.8%) and LIP (16.4%) (Fig. 3.5.1).

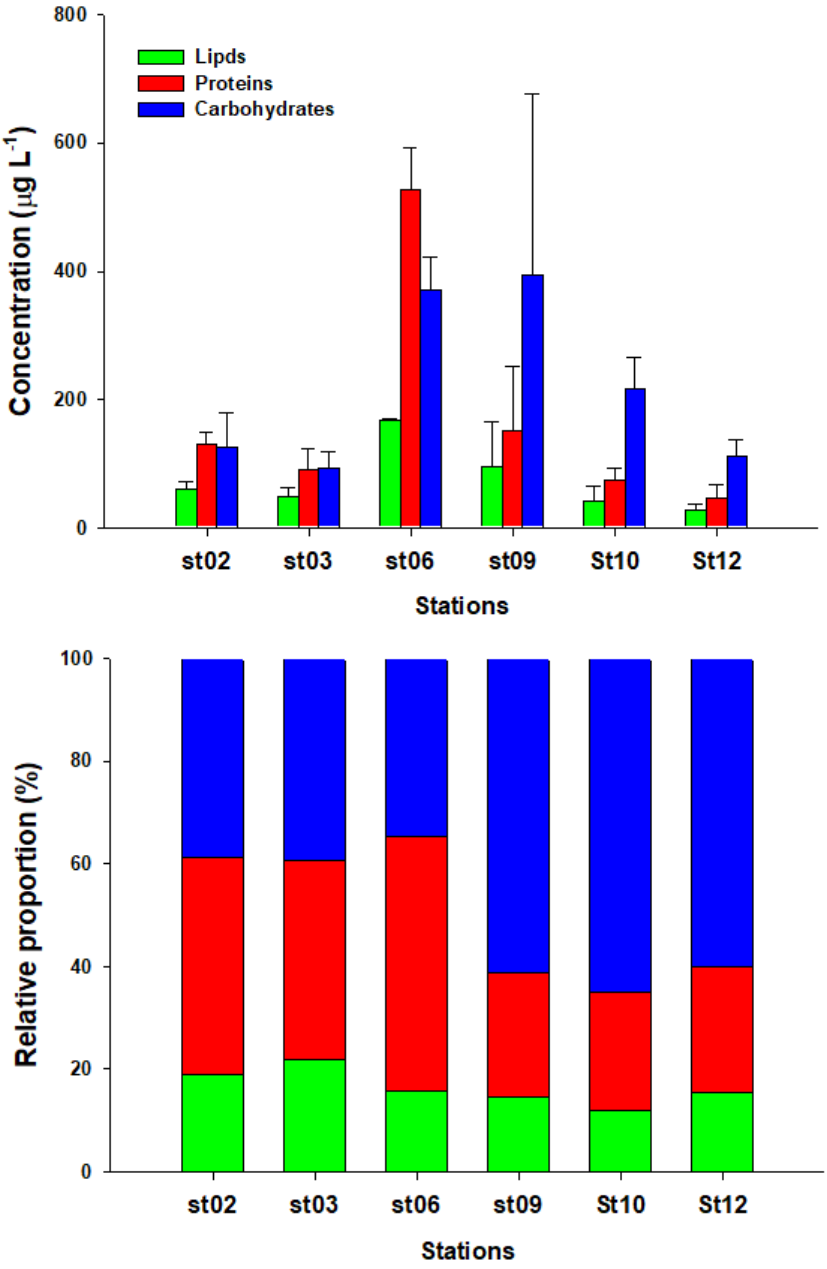

Figure 3.5.1. Macromolecular concentration and composition of phytoplankton.

6) Protozoa abundance, composition and grazing rates on phytoplankton

Data analysis in progress.

7) Mesozooplankton and Food web

Brief results are shown in figure 3.7.1. and Data analysis in progress.

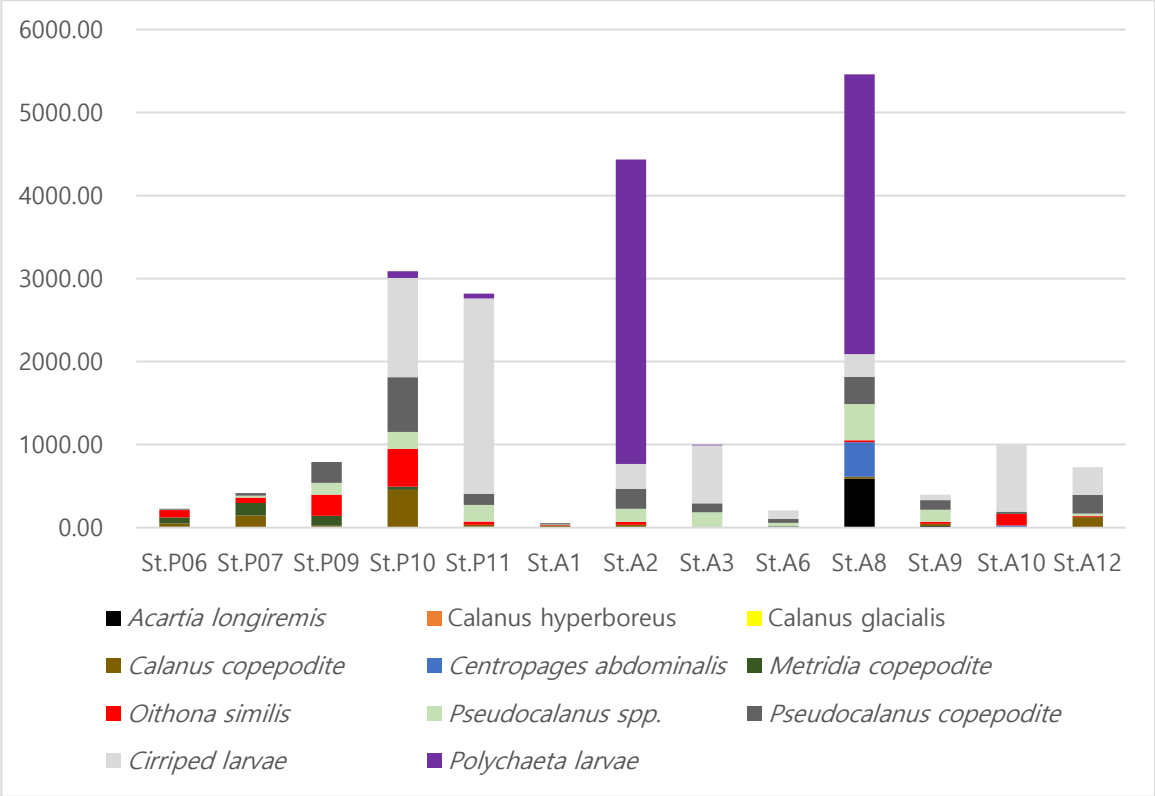

Figure 3.7.1. Zooplankton abundance per Unit Volume (indiv / m^3)

8) Ocean Optical Observation

The results from the IOPs will be able to show the bio-optical characteristics in water at each station and at each depth of the water sample (Fig. 3.8.1).

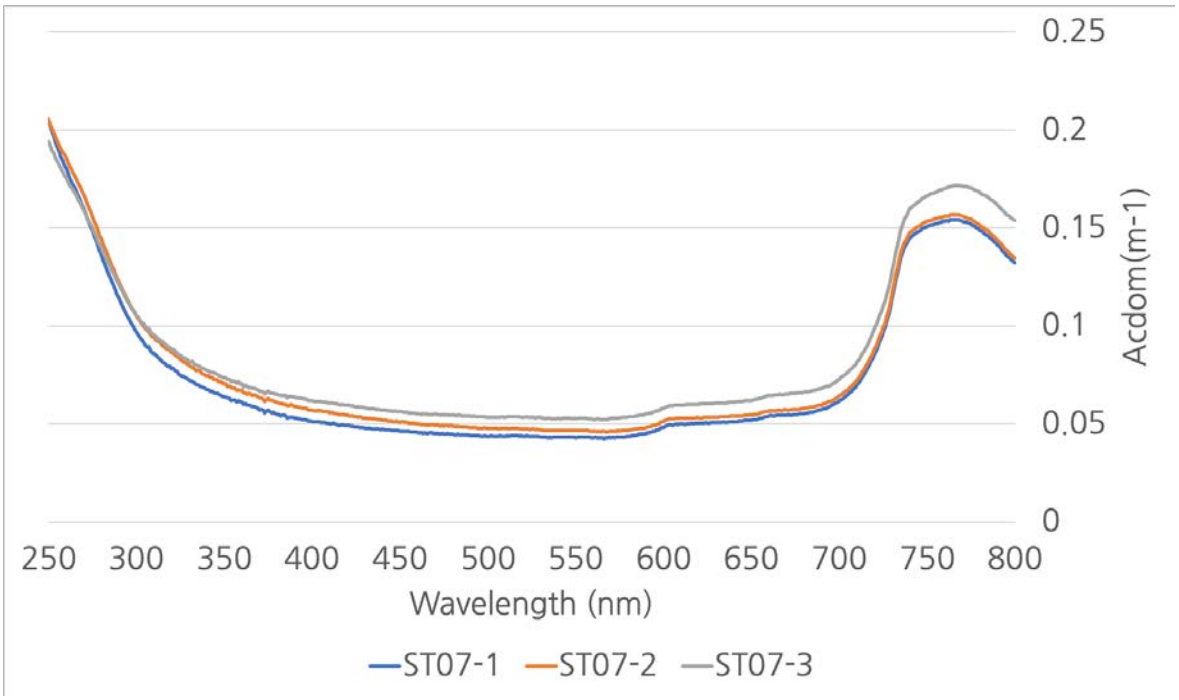

Figure 3.8.1. An example of absorption colored dissolved organic matter at the station 7.

During this Arctic cruise, data for calibration/validation of satellite remote sensing ocean color data were collected. The IOPs reflected the bio-optical characteristics in water at the selected depths. The results from the AOPs, i.e. data from HPRO II, reflect the continuous bio-optical characteristics of water surface and the bio-optical profiles at the operated station (Fig. 3.8.2). We are going to use these field data for further detailed examination and correction of satellite data.

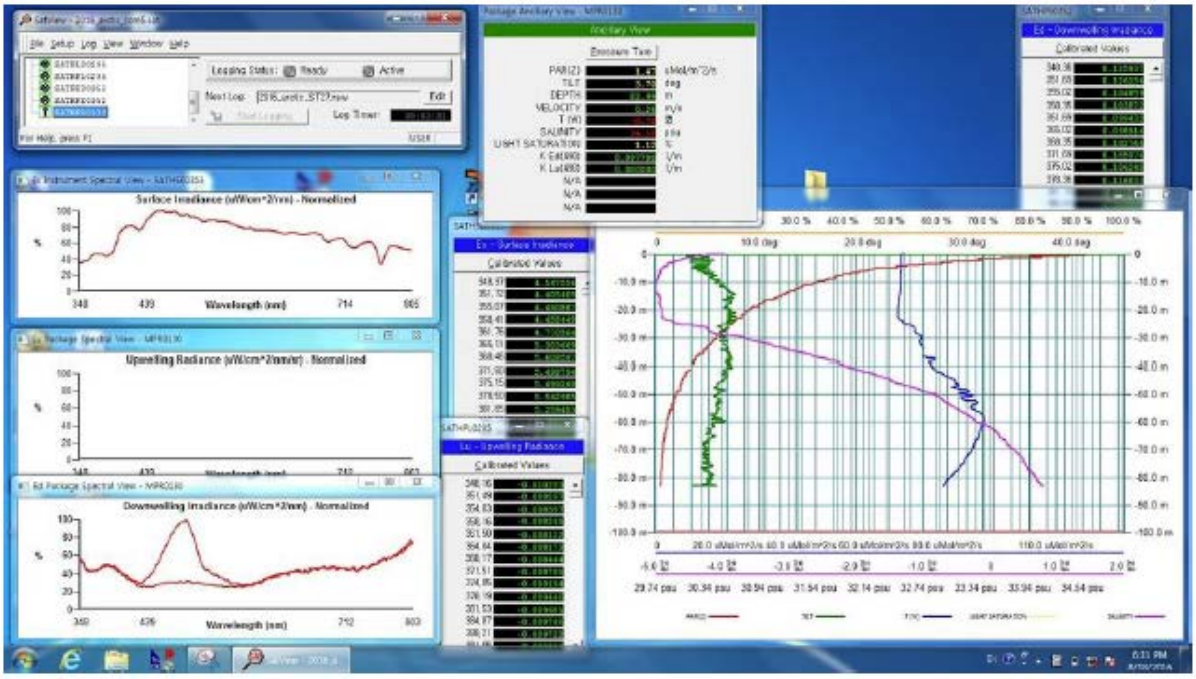

Figure 3.8.2. An example of HPRO II data signal recorded at the station 12.

9) Phytoplankton physiology (photochemistry)

Fig. 1.9.1 shows the station map and the average minimal fluorescence (F_0), quantum efficiency of PSII (F_v/F_m) and functional absorption cross section (σ_{PSII}) in the mixed layer. The minimal fluorescence parameter indirectly indicates the biomass of phytoplankton. The values of F_0 were higher in the Bering Strait than that in the Bering Sea and the southern Chukchi Sea. Based on F_o values, phytoplankton biomass in the Bering Strait was significantly different in the Bering Sea and the southern Chukchi Sea. The quantum efficiency of the Bering Strait and the southern Chukchi Sea was higher than 0.50 on average, whereas that of the Bering Sea was relatively low (< 0.45). This indicates that the nutrient limitation for phytoplankton photosynthesis is low in the Bering Strait and the southern Chukchi Sea. The functional absorption cross section ranged from 400 to 500 10^{-20} m^{-2} $photon^{-1}$ in the Bering Strait and the southern Chukchi Sea, but more than 600 10^{-20} m^{-2} $photon^{-1}$ at station P6 and P7 around the Bering Sea. Considering the trend with quantum efficiency, nutrient deficiency (mainly nitrate) in the upper layer of the Bering Sea resulted in relatively low quantum efficiency (0.41-0.45) and very high functional absorption cross section, which may be due to an increase in secondary pigment function (Chlorophyll-b or c) than chlorophyll-a pigment. On the other hand, the differences in phytoplankton community composition and size between the Bering Sea and Bering

Strait may have caused the differences in quantum efficiency and functional absorption cross section.

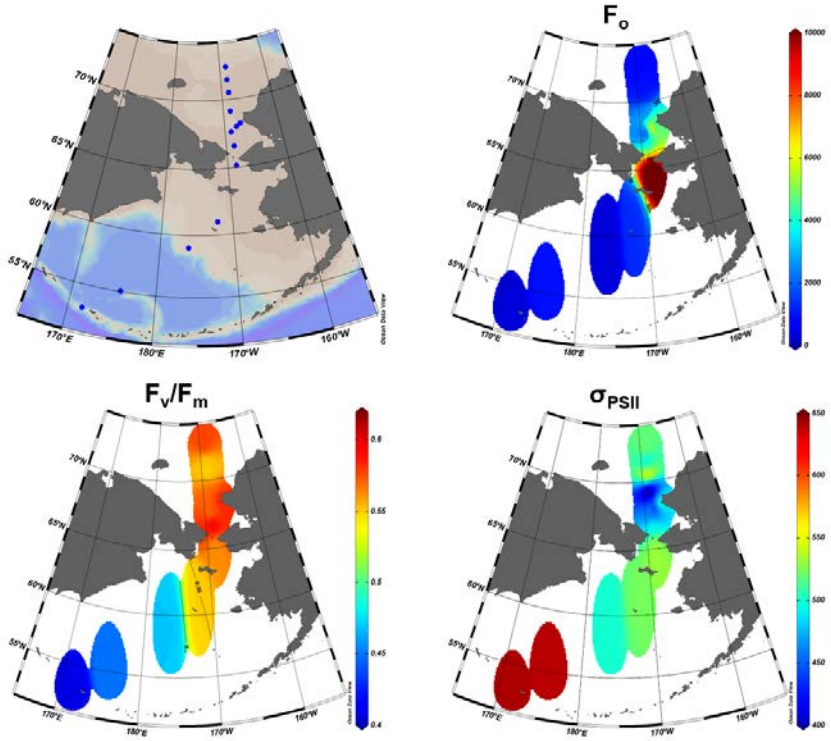

Figure 1.9.1. Station map and the spatial distribution of minimal fluorescence (F_0), quantum efficiency of PSII (F_v/F_m) and functional absorption cross section (σ_{PSII}, 10^{-20} m^2 $photon^{-1}$).

The above three fluorescence variables are shown as vertical distribution from station P10 to A12 (Fig. 1.9.2). The minimal fluorescence was highest at the surface near the Bering Strait, and the rest of the area was very low. The station P10 in the Bering Sea showed a relatively high F_o values below the surface, and F_o values in the station A10-A12 were also high at 30-40m. In other words, except for the surface of the Bering Strait, phytoplankton biomass was high below the surface. On the other hand, quantum efficiency and functional absorption cross section showed opposite trends. The quantum efficiency was above 0.5 in the Bering Strait and the southern Chukchi Sea, higher than that of Bering Sea (0.3-0.45). In addition, the functional absorption cross section in the Bering Sea was mainly 550-850 10^{-20} m^{-2} $photon^{-1}$, which was higher than 450-550 10^{-20} m^{-2} $photon^{-1}$ in the Bering Strait and the southern Chukchi Sea. This suggests that the phytoplankton physiological characteristics between the Bering Sea and the Bering Strait + southern Chukchi Sea are different.

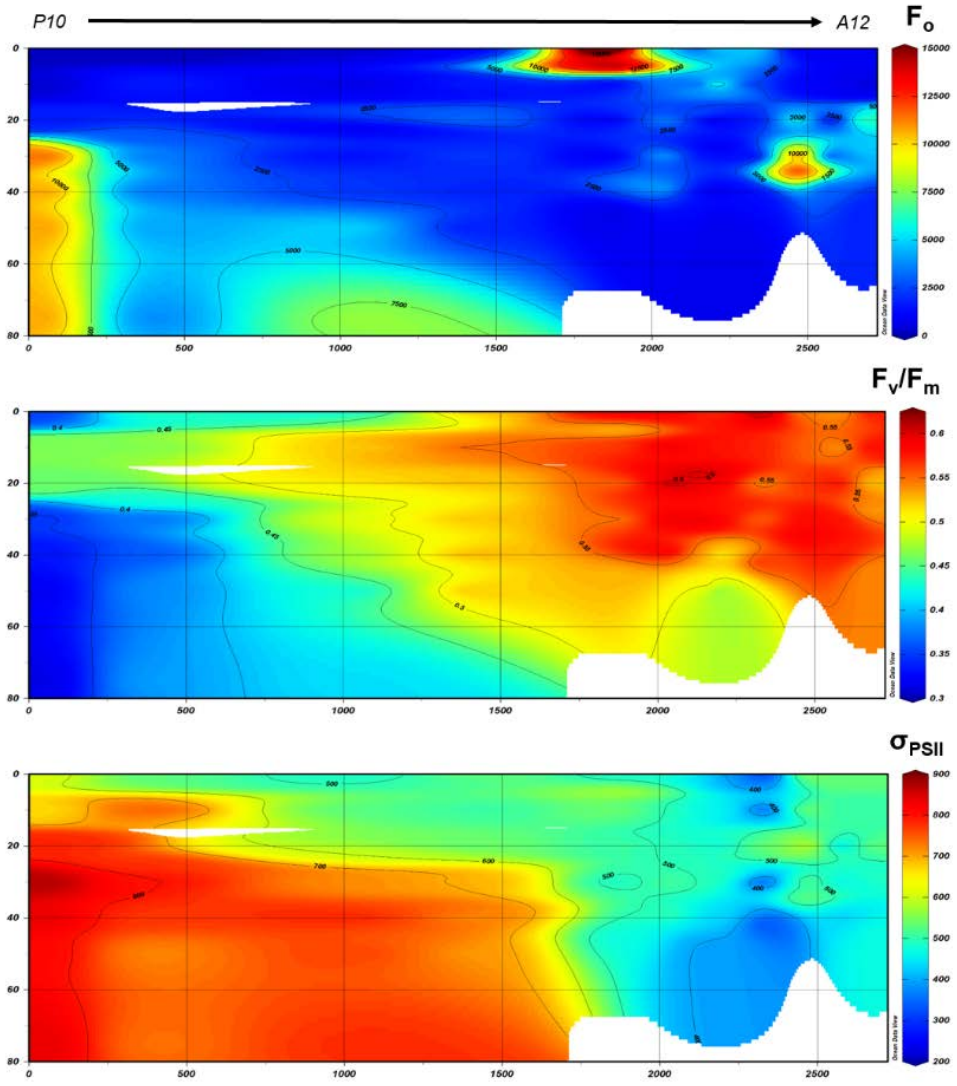

Figure 3.9.2. the vertical distribution of of minimal fluorescence (F_0), quotum efficiency of PSII (F_v/F_m) and functional absorption cross section (σ_{PSII}, 10^{-20} m^{-2} $photon^{-1}$).

10) UV absorbing compound (Mycosporine-like amino acids; MAAs) and light intensity

Data analysis in progress.

11) Nutrients and dissolved and particulate organic carbon and nitrogen in the Arctic Ocean

There was an east–west gradient in water-mass properties across stations 3–8, with

the highest nutrient concentrations, highest salinities, lowest temperatures generally occurring in the Anadyr Water in the west; and the lowest nutrient values, and lowest salinities and highest temperature tending to occur in Alaska Coastal Water in the east (Fig. 3.11.1). PO4 concentration varied from 0.25-0.75 μmol/L in the east side where the influence of Alaska Coastal Water is strong, whereas NO_2+NO_3 concentration was below detection limit, suggesting that primary production in the Arctic Ocean is limited by nitrogen. In contrast, nutrients concentration in the west, where the influence of Anadyr Water is strong, was high. Especially, NH_4 concentration varied from 0.5~5.5 μmol/L, which is derived from the decomposition of particulate organic matter, suggesting active decomposition of particulate organic matter by bacteria in the continental shelf.

For dissolved organic matters, the highest DOC concentration was observed in the eastern side where the influence of Alaska Coastal Water was strong, suggesting that DOC was mainly derived from terrestrial sources. DON showed somewhat different distribution to that of DOC. The POC showed a similar distribution to that of PON in the upper layer (0-20 m), but their distributions were different in the deeper layer, suggesting that POC and PON have different sources.

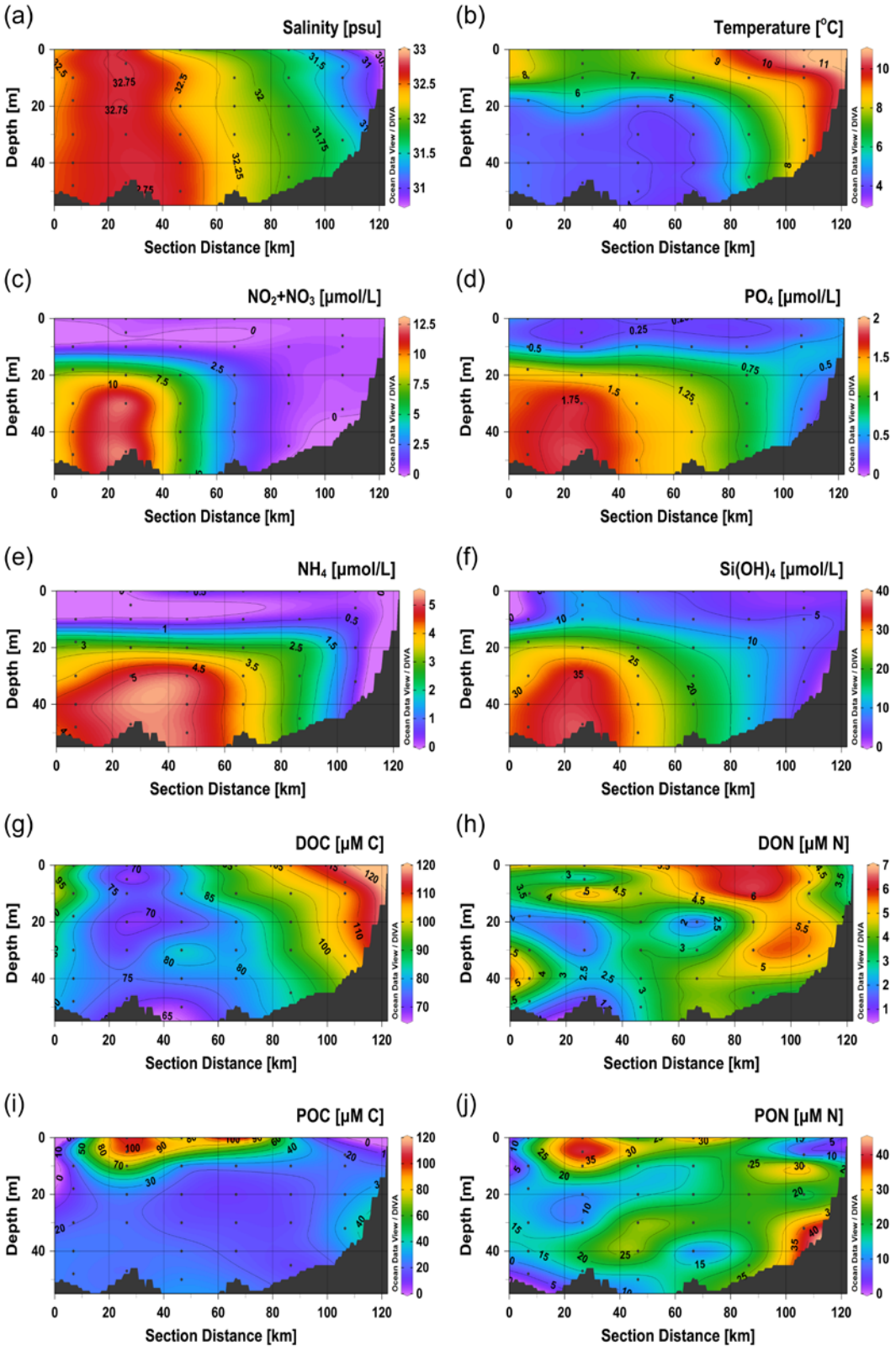

Figure 3.11.1. Salinity (a), temperature (b), PO_4 (c), NO_2+NO_3 (d), NH_4 (e), $Si(OH)_4$ (f), DOC (g), DON (h), POC (i) and PON (j) concentrations in a section taken from stations 3–8 during the ARA08B cruise.

12) Atmospheric black carbon and chemical properties of aerosols

Figure 3.12.1 shows time series of BC mass concentrations observed during the cruise in 2017. The BC concentrations were occasionally enhanced up to 10 μg/m^3, with the maximum concentration exceeding 40 μg/m^3. The majority of data fell in the range of 0 to 0.3 μg/m^3, with an average being approximately 0.05 μg/m^3. This is close to the instrument detection limit (~0.05), and needs further investigation of its significance. The O_3 concentrations were generally in the range from 20 to 40 ppbv, with occasional drops as low as near 0 ppbv, likely due to the contamination of the ship's exhaust. Here we scrutinized the BC data by using the O_3 data lower than 20 ppbv to be the data "possibly" contaminated by the ship's exhaust.

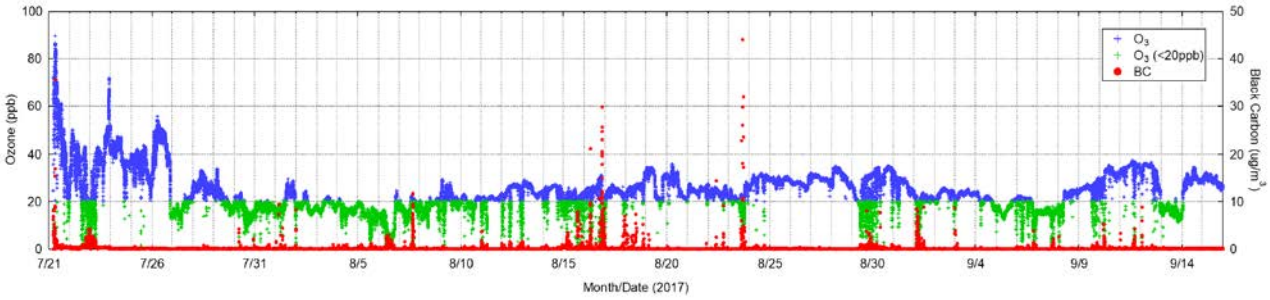

Figure 3.12.1. Time series of BC and O_3 during the 2017 Araon cruise.

Figure 3.12.2 shows time series of wind directions observed during the cruise in 2017. The wind direction varied a lot during the cruise, and we used the BC data that was not associated with the wind direction ranged from to 90 to 270 degrees, in order to make sure the BC data in "clean air" over the open ocean.

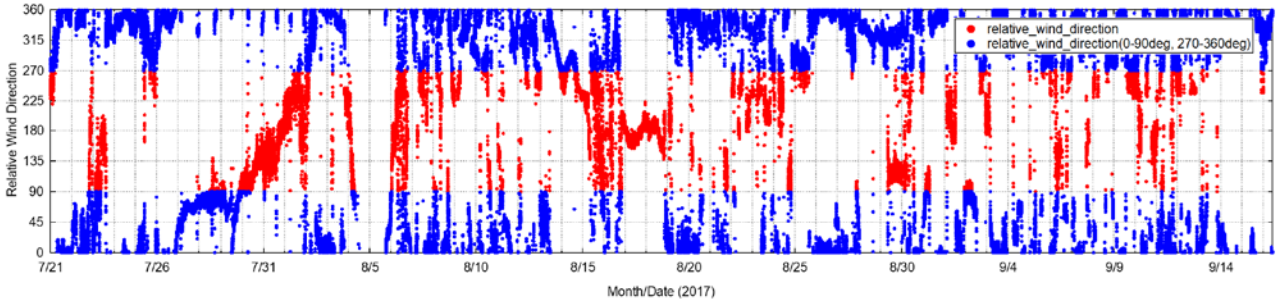

Figure 3.12.2. Time series of wind direction during the 2017 Araon cruise.

Figure 3.12.3 shows time series of BC and O_3 in “clean air” after careful selections with O_3 data (lower than 20 ppbv) and wind directions (90-280 degrees) observed during the cruise in 2017. The majority of BC data fell in the range of 0 to 0.3 μg/m^3, with an average being approximately 0.05 μg/m^3. The BC concentrations were occasionally enhanced up to 1 μg/m^3 over the open ocean but as high as 4 μg/m^3 near the Asian continent, just after the departure.

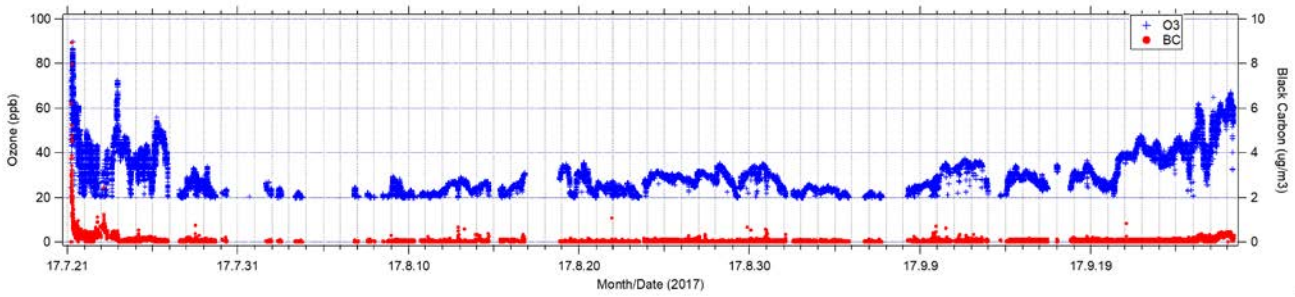

Figure 3.12.3. Time series of BC and O_3 in “clean air” during the 2017 Araon cruise.

13) Air-sea CO_2 exchange and water column carbonate system

The Arctic Ocean lies in the center of the current climate change as the summer sea-ice extent shrinks dramatically in recent years. Several modeling studies predict complete disappearance of the sea-ice extent in summer this century. One of the concerns resulting from this rapid change in the Arctic climate is the impact on the marine ecosystem in which carbon is the backbone of the energy flow initiated by solar energy. In addition, the shift of the ice-covered to the complete open ocean may lead to the change in the CO_2 flux across the sea-surface due to the imbalance in pCO_2 between, which is ultimately driven by the primary production in the surface mixed layer and by the Arctic circulation. To investigate the change in the air-sea CO_2 flux and the carbonate system interior of the water column, we have visited for 5 years the Chukchi Sea every summer season since 2010 and the Beaufort Sea in 2013 and 2014 onboard the Korean ice breaking R/V Araon. The areas surveyed were always undersaturated with respect to the atmospheric CO_2 despite large variability of the degree of saturation. We explored the spatial and temporal characteristics of the carbonate system in conjunction with the extent to which physical and biological properties would influence. To identify the driving forces in changing carbonate system interior of the water column, we focused on the impact of sea-ice

melting, freshwater input from the continent, enhanced biological uptake driven by primary production, and chemical processes, which allow us to delve carbon flow in these particular area. In the presentation we will discuss the results from the 5-year observations in the picture of the rapid change in the Arctic environment.

The figure 3.13.1 and figure 3.13.2 shows the observation results of pCO_2 measurement during 2017 arctic cruise and further analyses are undergoing now.

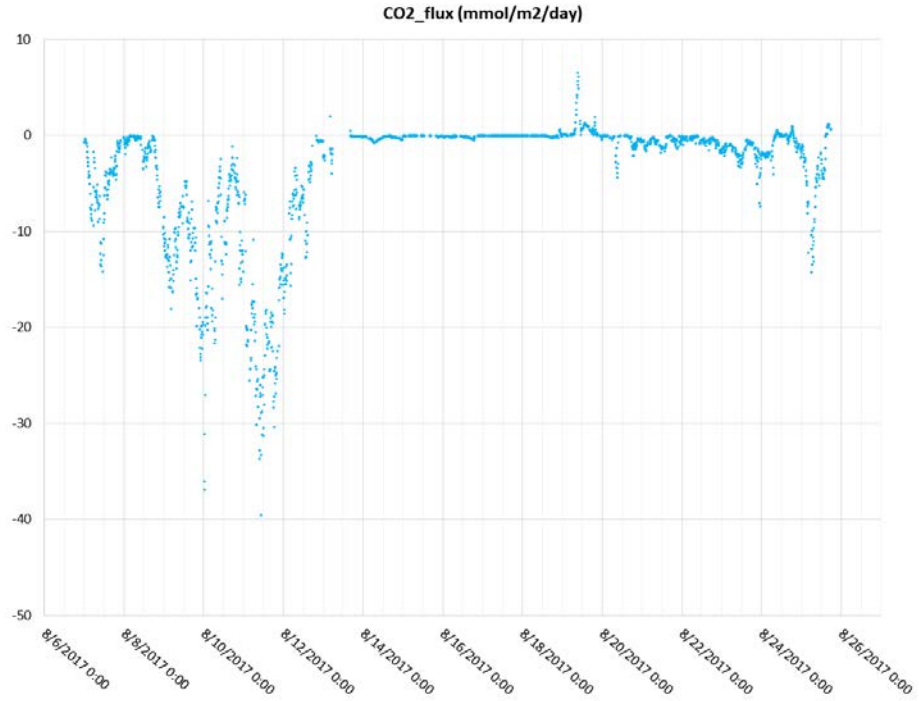

Figure 3.13.1. Timeseries of pCO_2 during ARA08B Cruise

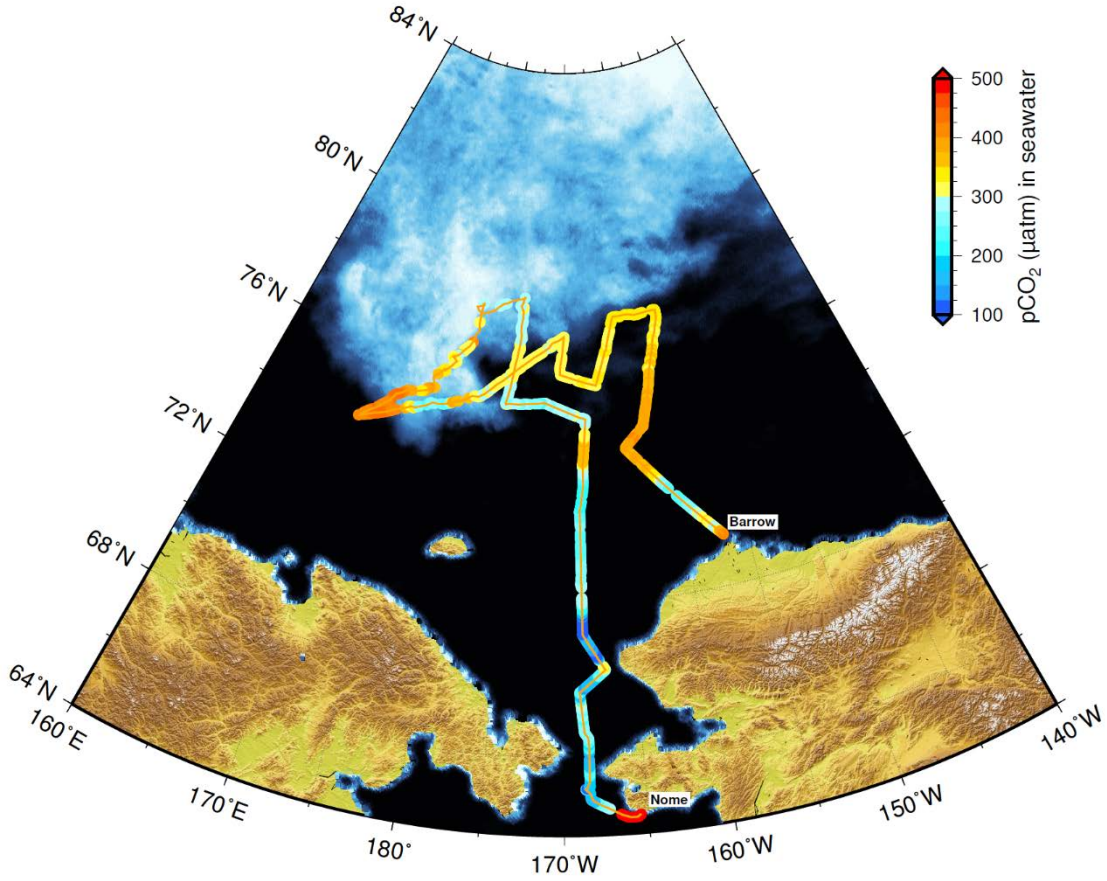

Figure 3.13.2. Spatial distribution of pCO_2 during the 2017 Arctic cruise

14) Investigation of the microplastic contamination in surface water

A total of eight samples collected from the US EEZ were analyzed to determine the spatial distribution of microplastic contamination in surface water. The analysis of microplastics was performed at > 100 µm using a microscope and FT-IR but considering the mesh size of the manta net, it is reasonable to measure MPs of > 200 µm.

The contamination level of the microplastics remaining in the eight surface waters analyzed was 0.22-1.02 (0.54 ± 0.31) n / m^3 including paint particle and 0.15–0.53 (0.28 ± 0.12) n / m^3 excluding paint particle. The various microplastics remaining in the Arctic surface water investigated in this study were observed. The most predominantly detected MPs were fragment paint-MP (48%), PET (49%), which forms MPs in the form of fiber is used for clothing. This means that the MPs pollutant in this area may be a vessel. And the results are different from those observed in sea water originating from the Atlantic Ocean. Therefore, the origin and migration route of MPs in the process of connecting the

Atlantic to Arctic and the Pacific to Arctic of this study need to be revealed through future studies. Excluding ship-based paints, PET was 95% dominant. Except for ST10, the concentration tends to decrease toward the north from the Bering Sea, suggesting the inflow of MPs through the Bering Sea. We are further examining the analysis data for their quality assurance.

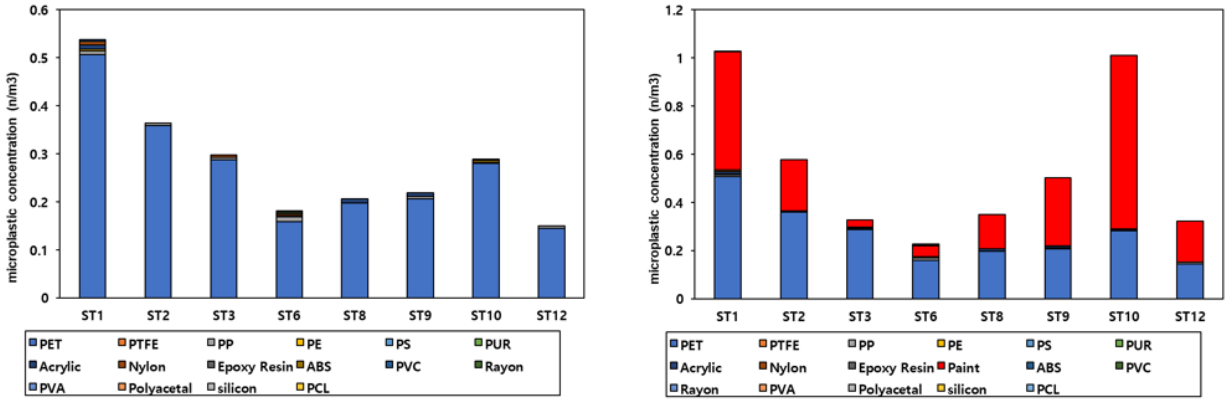

(a) Microplastic polymer type (excluding paint particle)　(b) Microplastic polymer type (including paint particle)

Figure 3.14.1. Distribution of microplastic type

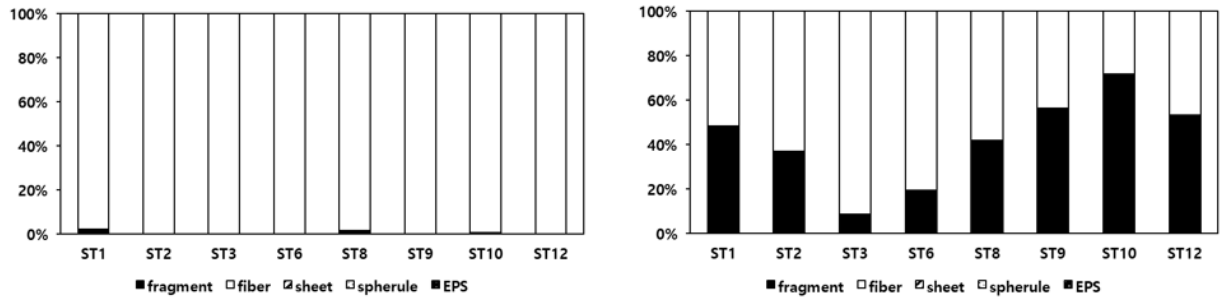

(a) Microplastic shape type (excluding paint particle)　(b) Microplastic shape type (including paint particle)

Figure 3.14.2. Contribution of microplastic Shape

15) Nitrogen source determination using nitrogen isotope of amino acids

Trophic position values of zooplankton were calculated using nitrogen isotope ratio of amino acids and nitrogen baseline values of primary producer were estimated by removing trophic enrichment factor of zooplankton (Fig. 3.15.1).

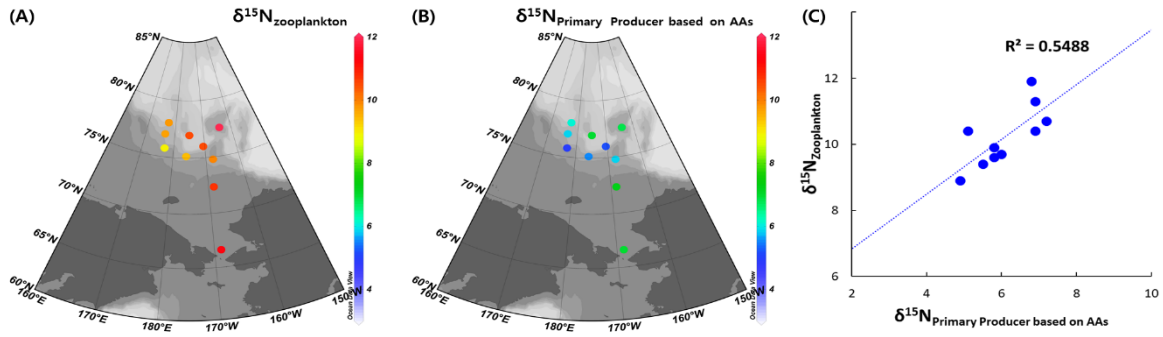

Figure 3.15.1. (A) bulk tissue $\delta^{15}N$ of zooplankton (‰), (B) nitrogen baseline of primary producer (‰), (C) the correlation between bulk tissue $\delta^{15}N$ and nitrogen baseline of primary producer

Oxygen isotope values were used to estimate contribution of water mass in seawater (Fig. 3.15.2).

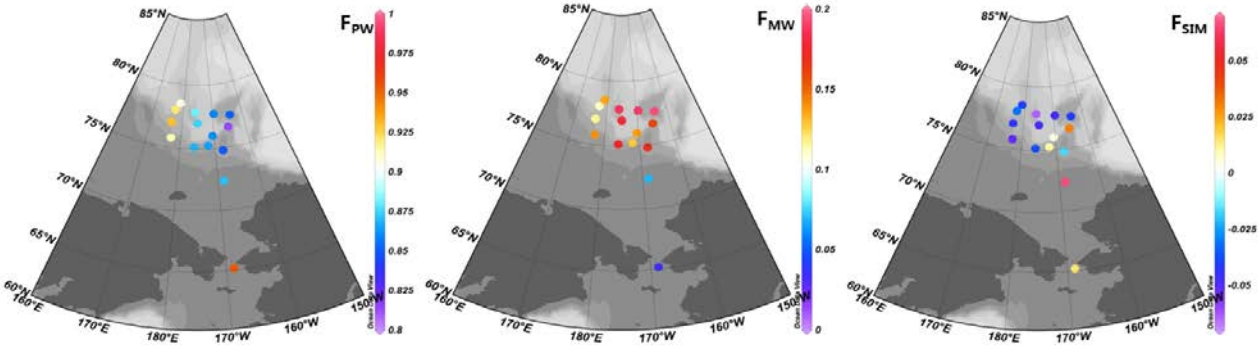

Figure 3.15.2. Water mass composition of Pacific water (A), Meteroric water (B), Sea-ice melted water (C)

16) Atmospheric Observations

The statistical distribution of true wind directions and speeds observed during the cruise are shown in Fig. 3.16.1 as a wind rose plot. In 2017, the northwesterlies prevailed and the maximum wind speeds were between 10-15 m/s.

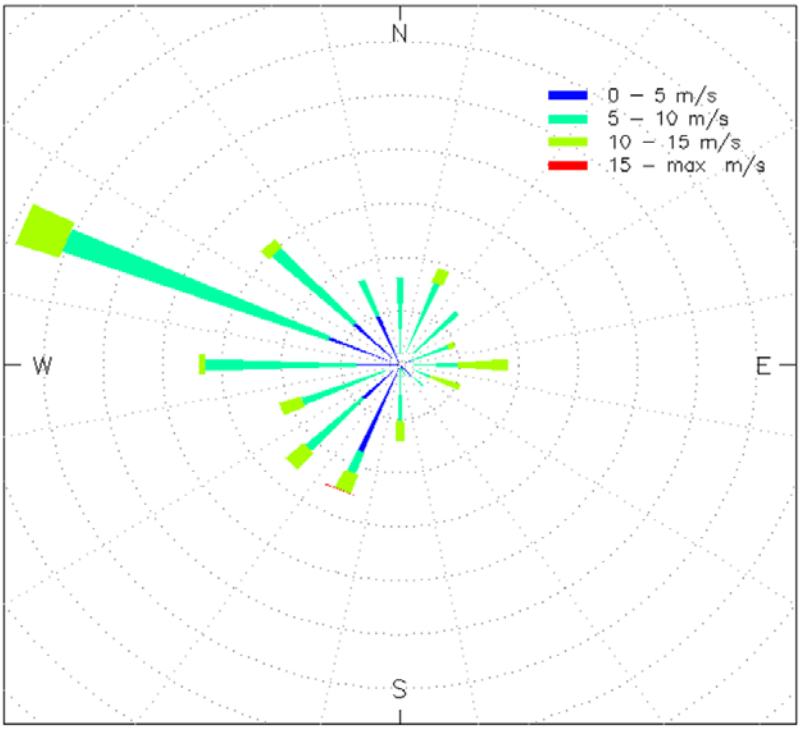

Figure 3.16.1. Distribution of wind directions and speeds during 2017 Araon Arctic expedition.

Air temperature records measured by HMP45D at the radarmast (38 meters ASL) are shown in Fig. 3.16.2 On the second and third days of cruise (August 2-3, UTC), IBRV Araon entered the Arctic Circle (north of 66°N) and continued cruising to the north. Air temperature dropped quickly below the freezing level while the vessel voyaged northeastward through the Chukchi Sea. Average air temperature in the Arctic was about -1°C and the minimum was about -3.8°C just prior to the sea ice camp.

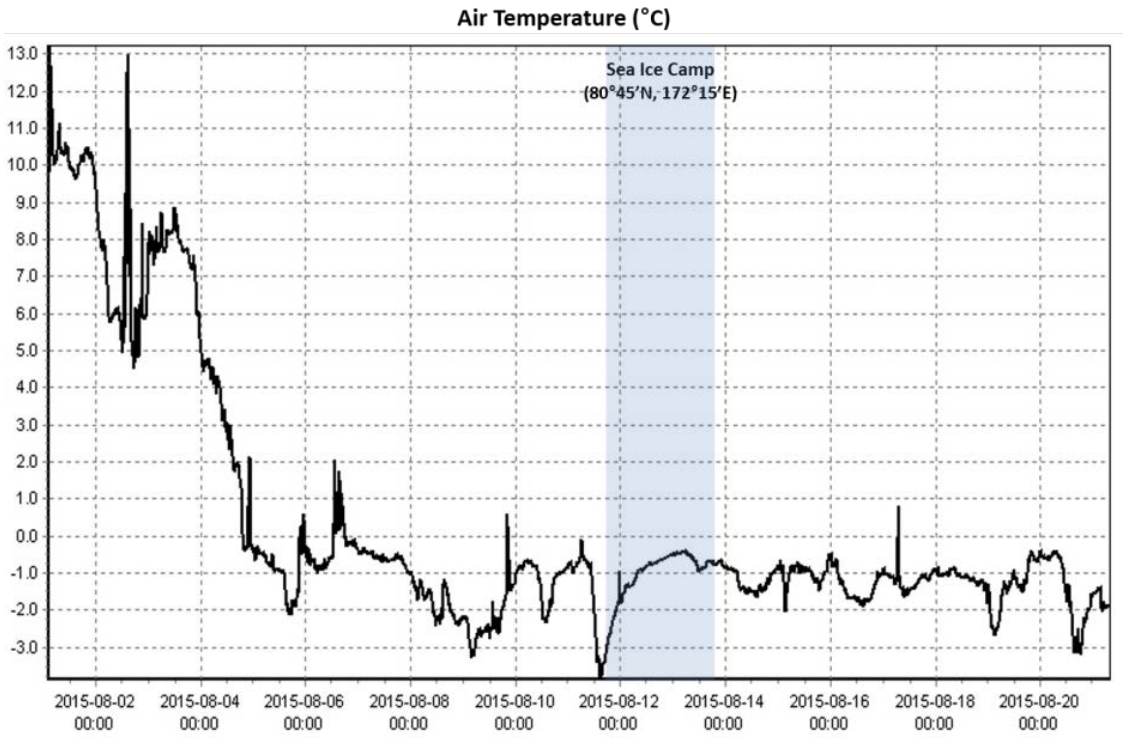

Figure 3.16.2. Time series of air temperature during 2017 Araon Arctic expedition.

3. Publications

We have not yet published papers in scientific journals out of the results from the expedition. However, several papers have been presented in various meetings held in domestic and foreign countries.